



Giant Mine Environmental Assessment

Technical Session Undertakings

EA No: 0809-001

November 14, 2011

UNDERTAKING RESPONSE

EA No: 0809-001

Undertaking No: 1

Date Received

Transcript: Day 1, pg. 259

Undertaking:

The Giant Mine Project Team to provide the Freeze Optimization Study interim report to the Review Board.

Response:

Please see attached report, *Freeze Optimization Study Interim Report*, November 14, 2011.



Giant Mine Freeze Optimization Study – Initial Findings (Final Draft)

Report Prepared for

Public Works and Government Services Canada



Report Prepared by



SRK Consulting (Canada) Inc.
1CS019.018
November 2011



Giant Mine Freeze Optimization Study – Initial Findings (Final Draft)

Public Works and Government Services Canada

5101 50th Avenue, P.O. Box 518, Greenstone Building
Yellowknife, NT X1A 2N4

SRK Consulting (Canada) Inc.
Suite 2200 – 1066 West Hastings Street
Vancouver, BC V6E 3X2

e-mail: vancouver@srk.com
website: www.srk.com

Tel: +1.604.681.4196
Fax: +1.604.687.5532

SRK Project Number 1CS019.018

November 2011

Executive Summary

The Freeze Optimization Study has been in operation since early March 2011. Active freezing Groups A, C, M and the underground freeze pipes were activated at that time, with Groups E and H activated in late May. Of the hybrid thermosyphons, Group B was operated actively since early March, while Groups F and G were operated passively from March to May 25, and then switched to active operation. Freeze pipes in areas where drift plugs are to be installed underground (Groups D, J, K and L) have yet to be activated.

Even without the activation of freeze pipes at the northern and southern ends of the study, the 0°C isotherm has surrounded Chamber 10 on all sides. The ground around the active freeze pipes is cooling more rapidly than estimated in the Remediation Plan. The quicker cooling is thought to be a result of the bedrock thermal diffusivity being higher than previously estimated.

Key results from operation of the Freeze Optimization Study to date are:

- The freezing systems have been installed and commissioned and are in operation
- Inspection of drill core from eleven holes around Chamber 10 indicates that variation in mineral composition of the rock has an effect on thermal conductivity. The typical thermal conductivity at the FOS is estimated at $400 \text{ kJ m}^{-1} \text{ day}^{-1} \text{ }^{\circ}\text{C}^{-1}$, but could range from 230 to $485 \text{ kJ m}^{-1} \text{ day}^{-1} \text{ }^{\circ}\text{C}^{-1}$.
- Freeze pipe diameter has been observed to have little effect on performance of either active freeze pipes or thermosyphons. The 3 inch active freeze pipes are performing as well as 4 inch pipes. For the thermosyphons, there is negligible difference in performance between Group F with 4 inch pipes and Group G with 2.5 inch pipes.
- Comparisons of freezing technologies have been made for active freezing, hybrid thermosyphons operating in passive mode, and hybrid thermosyphons operating in hybrid mode.
- Instrumentation readings as a measure of instrumentation reliability indicate that defective readings can occur during installation of temperature sensors in the ground, during initial freezing and during ongoing freezing.
- The data historian and monitoring system read information from the data capture systems housed in the instrumentation building and freeze plants. Reconciliation of monitoring data on the historian is ongoing as the data provided are in some cases different from what is available on the programmable logic controllers.
- Methods have been developed to estimate thermal conductivity, thermal diffusivity, heat transfer coefficient and heat flux for the rock around Chamber 10.
- 2 -D and 3-D models have been developed. The models are based on estimates of rock properties, estimates of heat transfer rates and actual data.
- The time to establish a frozen shell has been estimated for active freeze pipes and thermosyphons. The sensitivity to pipe spacing and distance of freeze pipes from the chamber were considered.

- At the Startec plant, power usage data from the programmable logic controllers do not agree with data on the motor control centre. The power data are under investigation by AECOM.
- The Coefficient of Performance (COP) is a measure of cooling system efficiency, and is the ratio of estimated heat extraction to measured power input. Higher ratio values indicate better performance. The active operation COP to date for the Arctic Foundations of Canada Inc. freeze plant has ranged between 1.0 and 1.3 when all hybrid thermosyphons are operating. These values do not include passive heat removal. The COP for the Startec freeze plant has not been finalized due to the uncertainty in the power consumption records.

Continuing operation of the Freeze Optimization Study will provide information not available to date:

- The operation of the hybrid thermosyphons has not been tested in cold weather under optimal performance. Data from the coming winter will provide information about passive operation with and without mechanical assistance from the heat exchange coils.
- The Group D, J, K and L freeze pipes are in areas where drift plugs will be installed on first and second levels underground. Their activation is dependent on the design and installation of the plugs. The drift plug design and field trials were partially completed by SRK in 2009 and 2010. In 2010, AECOM became responsible for plug design and installation which is still in progress.

Table of Contents

1	Introduction	1
2	Background	2
3	Freeze Pipe Layout	3
3.1	Group Descriptions	4
3.1.1	Active Freezing	4
3.1.2	Hybrid Thermosyphons	5
3.2	Activation Sequence	5
4	Study Timeline	7
5	Performance Monitoring.....	9
5.1	Monitoring of Ground Temperatures.....	9
5.2	Climate Monitoring	9
5.3	Monitoring of Individual Freeze Pipes.....	9
5.3.1	Active Freeze Pipes	9
5.3.2	Hybrid Thermosyphons	10
5.4	Monitoring of Freeze Groups	12
5.5	Monitoring of Distribution Loops	12
5.6	Monitoring of Freeze Plant Performance	13
6	Data Management and Data Handling Methods	14
6.1	Data Management and Collection Frequency	14
6.2	Data Collection Issues and Recommendations	16
7	Ground Freeze Progress to September 2011	18
8	Study Evaluation	21
8.1	Estimation of Parameters Needed for Design	21
8.1.1	Bedrock Thermal Conductivity	21
8.1.2	Bedrock Thermal Diffusivity.....	24
8.1.3	Arsenic Thermal Conductivity	29
8.1.4	Power Requirements.....	29
8.1.5	Freeze Plant COP	30
8.1.6	Active Heat Transfer Coefficients.....	32
8.2	Hybrid Thermosyphon Pipe Diameter.....	36
8.3	Passive Thermosyphon Heat Flux	38
8.3.1	Comparison of Predicted Flux Formulas.....	38
8.3.2	Comparison of Predicted Flux to 2D Model, Groups F and G	39
8.3.3	Thermosyphon Heat Transfer Coefficient	41
8.4	Active Freeze Pipe Diameter and Completion Detail Comparison	42

8.5	Comparison of Active Freezing and Hybrid Thermosyphon Performance	44
8.6	Group E Conversion.....	46
8.7	Time Predictions for Initial Freeze Wall Criteria.....	46
8.7.1	Model Setup	47
8.7.2	Effect of Arsenic Chamber Offset.....	51
8.7.3	Effect of Pipe Spacing	52
8.8	Instrumentation Reliability	54
8.8.1	Thermistors	54
8.8.2	Vibrating Wire Piezometers.....	55
8.8.3	Flow Meters	55
8.8.4	Resistance Temperature Detectors (RTDs).....	55
8.8.5	Power Meters	56
9	Summary of Findings to Date	56
9.1	Data Management.....	56
9.2	Ground Freeze Progress	56
9.3	Design Parameters	57
9.4	Comparison to Study Objectives.....	58
10	References.....	62

List of Tables

Table 3-1: Active Freeze Pipe Configurations.....	5
Table 3-2: Hybrid Thermosyphon Configurations.....	5
Table 5-1: Comparison of Thermosyphon Performance Coefficients	11
Table 6-1: Data Collection Frequency Rankings – Up to May 9, 2011	15
Table 7-1: September 8, 2011 Freeze Wall Thickness by Group	19
Table 8-1: Bedrock Sample Mineralogical Composition.....	21
Table 8-2: Bedrock Sample Thermal Conductivities	22
Table 8-3: Arsenic and Bedrock Physical Properties	24
Table 8-4: Estimated Range of Bedrock Thermal Diffusivity.....	25
Table 8-5: Theoretical Heat Transfer Coefficients for Three and Four Inch (J55) Pipes	33
Table 8-6: Heat Transfer Coefficient Summary	34
Table 8-7: Group E Average Dynalene Temperatures – Sept 2011	35
Table 8-8: Comparison of Predicted Thermosyphon Heat Flux	41
Table 8-9: Pipe Temperature Boundary Condition Parameters for Freeze Wall Time Prediction Modeling...	49
Table 8-10: Effect of Arsenic Chamber on Predicted time to reach -10 °C criterion (months)	51
Table 8-11: Effect of Pipe Spacing on Predicted time to reach -10 °C criterion (months)	52
Table 9-1: Comparison to Study Objectives	58

List of Figures

Figure 3-1: Freeze Pipe and Instrumentation Hole Layout	4
Figure 4-1: FOS Operation Timeline	8
Figure 5-1: Hybrid Thermosyphon Schematic.....	11
Figure 5-2: Thermosyphon Heat Flux Formula Comparison	12
Figure 6-1: Startec_PLC.FE_500 Data Collection Histogram	16
Figure 6-2: Data Collection Error Example – PT_M01_041, May 9, 2011	17
Figure 7-1: Freeze progress up to September 8, 2011.	19
Figure 7-2: Underground freeze progress up to September 8, 2011	20
Figure 8-1: Bedrock Lithology and Thermal Conductivities.....	23
Figure 8-2: Comparison of Modeled Temperature Responses for Groups A, B, F and G	26
Figure 8-3: Bedrock Diffusivity Model Calibration Results	27
Figure 8-4: Modeled Temperature Responses at S07 for Various Bedrock Thermal Diffusivities.....	28
Figure 8-5: Modeled Temperature Responses at S03 for Various Bedrock Thermal Diffusivities.....	29
Figure 8-6: Arctic Foundation and Startec Plant Power Consumption.....	30
Figure 8-7: Startec Plant Coefficient of Performance Versus Time	31
Figure 8-8: Arctic Foundations Plant Coefficient of Performance Versus Time	32

Figure 8-9: Heat Transfer Coefficient Calculations	34
Figure 8-10: P38 - Heat Transfer Coefficient versus Time.....	35
Figure 8-11: Hybrid Thermosyphon Performance Comparison of Groups F and G During Passive Operation.....	37
Figure 8-12: Hybrid Thermosyphon Performance Comparison of Groups F and G During Active Operation	37
Figure 8-13: Passive Thermosyphon Heat Flux – Group F.....	38
Figure 8-14: Comparison of Temperature Responses for Modeled and Theoretical Passive Thermosyphon Heat Flux.....	39
Figure 8-15: Comparison of Modeled to Theoretical Passive Thermosyphon Heat Flux.....	40
Figure 8-16: Passive Thermosyphon Heat Transfer Coefficients	42
Figure 8-17: Comparison of Active Freeze Pipe Temperatures	43
Figure 8-18: Comparison of Active Freeze Pipe Heat Flux.....	44
Figure 8-19: Comparison of Group A and Group B Pipe Temperatures	45
Figure 8-20: Comparison of Group E and Group F Pipe Temperatures	45
Figure 8-21: Comparison of Active Versus Hybrid Heat Flux (Group A and Group B)	46
Figure 8-22: Schematic Plan View of the Horizontal Plane Used as the Domain for the Thermal Simulations.....	48
Figure 8-23: Comparison of measured and modeled pipe temperatures for P01	50
Figure 8-24: Comparison of modeled pipe temperatures.....	50
Figure 8-25: Freeze wall thickness versus time with and without 7 m chamber offset and without.....	52
Figure 8-26: -10°C Freeze wall thickness for different pipe spacing.....	53
Figure 8-27: Thermistor Reliability Assessment.....	54

Appendices

- Appendix A: Drill Core Analysis Report
- Appendix B: Underground Photographs
- Appendix C: Additional Memorandum

1 Introduction

SRK Consulting (Canada) Inc. has assisted with the planning, construction and operation of the Freeze Optimization Study (FOS) at the Giant Mine Remediation Project in Yellowknife, NT.

The preparation and construction of the freeze systems are described in the Interim As-Built Report (2010a) by SRK and the as-built drawings provided by AECOM Technology Corporation. The FOS was initiated in late February and early March of 2011. The ground freezing systems have been in operation since that time with selected freeze technologies being activated in a predetermined sequence and schedule.

This initial findings report provides assessment and evaluation data derived from the FOS operation. The report presents operational results to date which provide direction for optimizing design aspects for the full freeze program at the site. Aspects of the study relating to the site as a whole and the site Remediation Plan are not the discussed in this report.

The study will continue in the shorter term with changes to the operating mode of some freeze groups and activation of the remaining freeze pipes. As the study continues, more will be learned about freeze variant performance, drift plug installation methods, the effects of freezing on drift plugs and options for improving freeze plant operations.

2 Background

A major component of the site Remediation Plan is to isolate the arsenic trioxide dust that is stored underground at the Giant Mine Remediation Project. Processing of the Giant Mine gold ore created arsenic trioxide dust as a by-product. Approximately 237,000 tonnes of the dust were produced and stored underground in fifteen stopes and purpose-built chambers. The dust is about 60% arsenic. To prevent the release of arsenic into the groundwater around the mine, the Remediation Plan calls for the arsenic trioxide dust and the rock around each stope and chamber and to be frozen. The method for doing this is known as the “frozen block method.”

Background details into why ground freezing is required as part of the site remediation work and the need for an optimization study are covered in the Interim As-Built Report (2010a) by SRK. Engineering assessments and thermal modeling completed in support of the Remediation Plan have shown that the frozen block method is technically feasible. However, additional information is needed before an optimum design can be developed. The FOS was designed to gather that information, and has been providing operating data since early March 2011. SRK has performed evaluations and assessments of the data, and presented its findings in this report.

Activities completed prior to operation of the study are presented as background information in the FOS. Once preliminary planning for the study was underway, civil works for site preparation commenced. Issues with sampling and segregation of contaminated material as well as working around unknown location of subsurface bedrock were resolved when bedrock was encountered. Methods and procedures for drilling to install freeze pipes and instrumentation pipes using three different types of drilling technologies have been demonstrated. The drills also installed thermistor strings on the outside of instrumentation and many of the freeze pipes. Thermosyphon installation included testing for leaks at pipe joints and charging with carbon dioxide. Drilling into and through voids was demonstrated. All activity was integrated with the site care and maintenance contractor's policies and procedures for environment, health and safety. Ancillary infrastructure design and installation included a dedicated electrical substation. Design of facilities on surface and underground as central locations for instrumentation terminations and data management were designed and mostly installed. Once the facilities were in place, start-up and commissioning were carried out and the system began operation.

The results of operation to date are the subject of this report. The continued operation of the FOS will inform other decisions required over the next few years. These will include technical and non-technical decisions about how to procure the freezing system and how to collect and manage performance monitoring data.

3 Freeze Pipe Layout

The layout of the freeze pipes installed from the surface is shown in Figure 3-1. There are a total of 38 vertical freeze pipes surrounding Chamber 10. The pipes are grouped according to the freeze method, size of pipe, in-hole installation arrangement and whether adjacent pipes are connected in serial or parallel. The vertical freeze pipes were labelled Group A to M; there is no Group I.

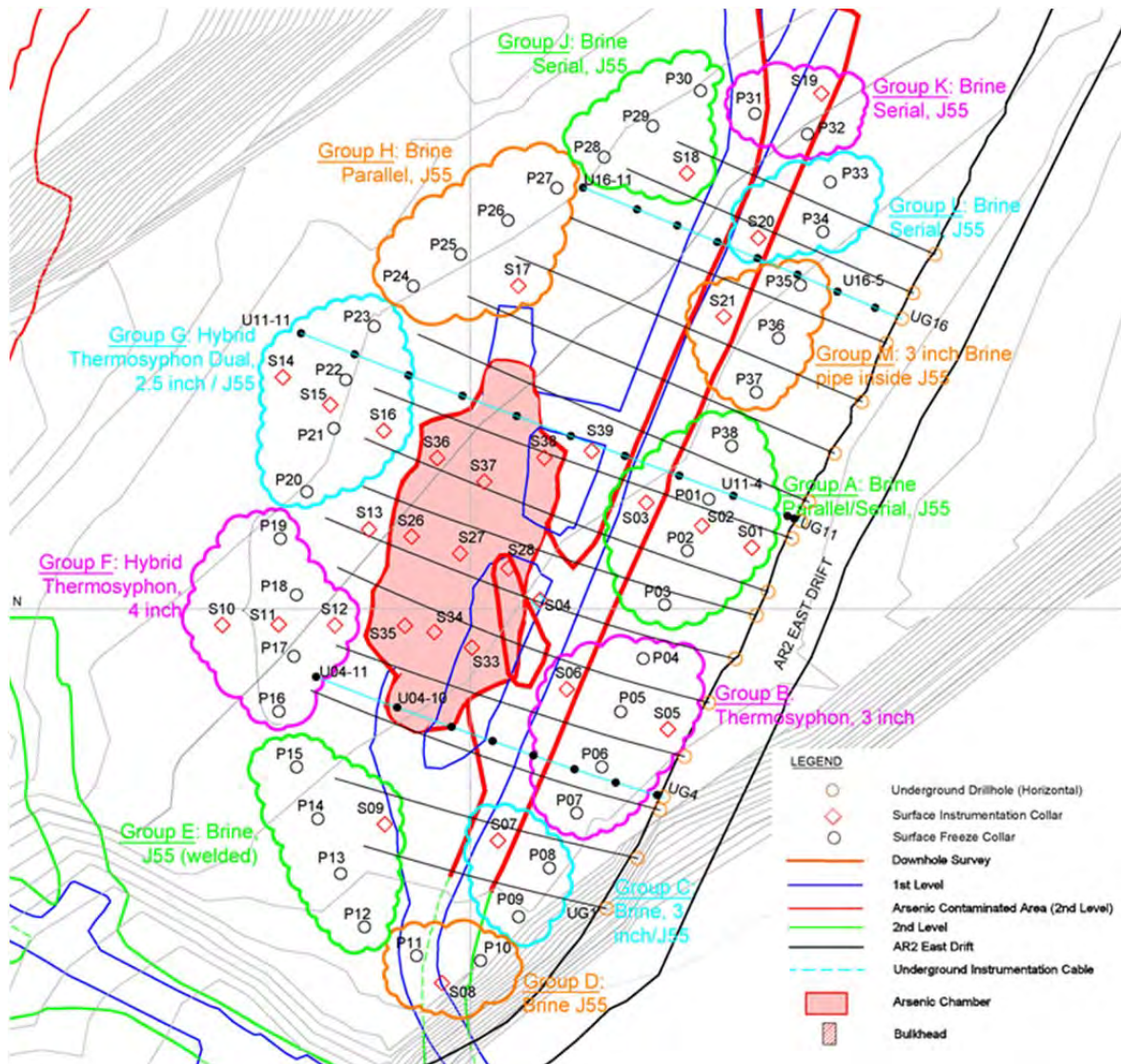
The reason for grouping the pipes is to be able to effectively assess performance for the possible range of installation combinations. The variants for active freeze pipes are with respect to connection arrangement, i.e., series or parallel and pipe diameter. Similarly, the hybrid thermosyphons were grouped with respect to variations in pipe diameter and in-hole installation arrangement.

The freeze pipe groups are arranged so that groups for comparison are next in line to each other. The main groups for comparison are A/B and F/G which are adjacent the chamber. Boundary conditions for each of these pairs are similar with an active freeze group on each end: on the east loop, Groups C and M close off Groups A/B while on the west loop, Groups E and H close off Groups F/G. Section 3.2 describes how the activation sequence for the groups will provide the data required for evaluation of individual groups and comparative evaluation between groups.

There are two dedicated freeze supply and distribution systems: one for the active freeze pipes that is operated by the Startec freeze plant, and one for the hybrid thermosyphons that is operated by the AFCI plant. Each plant operates as a separate stand-alone system to isolate the power usage and energy transfer data for itself. This avoids the possible confusion over allocating the data between the two systems, and provides a clear basis of assessment for and between each system.

Thermosyphon groups B, F and G are located adjacent to Chamber 10. The remaining active freeze pipe groups fill in the remaining perimeter of freeze pipes surrounding the chamber, including Group A, which is the fourth group adjacent to the chamber.

The layout of the underground horizontal freeze pipes installed from the AR2 East Drift is shown in Figure 3-1. There are a total of 15 underground freeze pipes connected in parallel. Holes for the horizontal pipes were drilled with a design dip of -3 degrees. Actual dips ranged from -3.5 to -8.7 degrees. The holes are positioned to prevent the possibility of hitting and damaging the vertical freeze pipes. On the east side of Chamber 10, they pass between the vertical freeze pipes, and on the west side, they were terminated typically 2 m short of the vertical freeze hole alignment. The pipes range in length from 31.2 m (U08) to 17.4 m (U01) with the longer pipes being directly beneath the chamber and the shorter pipes being north and south of the chamber.



Source File: Instrumentation Hole Layout.pptx

Figure 3-1: Freeze Pipe and Instrumentation Hole Layout

3.1 Group Descriptions

3.1.1 Active Freezing

At Chamber 10, four variations of active freezing are included in the study:

- 4.5 inch freeze pipe
- 3 inch freeze pipe inside 4.5 inch casing
- Parallel connection between pipes
- Serial connection between pipes

J55 casing was used for all active freeze pipe installations. The groupings and intended combinations of active freeze pipes are summarized in

Table 3-1.

Table 3-1: Active Freeze Pipe Configurations

Group	No. of Pipes	Freeze Pipe Size	Configuration
Group A	4	4.5" (114 mm)	Two serial pairs connected in parallel
Group C	2	3.0" (78 mm) inside 4.5" (114 mm)	Parallel connections
Group D	2	4.5" (114 mm)	Parallel connections
Group E	4	4.5" (114 mm)	Parallel connections
Group H	4	4.5" (114 mm)	Parallel connections
Group J	3	4.5" (114 mm)	All pipes connected in serial
Group K	2	4.5" (114 mm)	All pipes connected in serial
Group L	2	4.5" (114 mm)	All pipes connected in serial
Group M	3	3.0" (78 mm) inside 4.5" (114 mm)	Parallel connections
Underground	15	3.0" (78 mm)	Parallel connections

3.1.2 Hybrid Thermosyphons

Three Groups of thermosyphons were installed with four thermosyphons per Group. The Groups are identified as B, F and G in Figure 3-1. All thermosyphons are a hybrid design with two heat exchange coils (Coil A and B) located inside the pipe between ground level and the condensers. The location is evident where there is a widening of the thermosyphon pipes in the section between the ground and the radiators.

All thermosyphon assemblies were fabricated and installed by Arctic Foundations of Canada Inc. AFCL, including the straight runs, sections with heat exchangers and the condensers. The freeze plant and refrigerant distribution system was also supplied by AFCL.

The three variants of thermosyphons installed are summarized in Table 3-2.

Table 3-2: Hybrid Thermosyphon Configurations

Group	No. of Pipes	Freeze Pipe Size	Configuration
Group B	4	3.0" (80 mm)	Thermosyphon pipes grouted into a raw hole
Group F	4	4.0" (100 mm)	Thermosyphon pipes grouted into a raw hole
Group G	4	2.5" (65 mm)	Thermosyphon pipes grouted into a 4.5" (114 mm) J55 casing which was itself previously grouted into a raw hole

3.2 Activation Sequence

Sequencing the start-up of the freeze groups was planned in a manner that would best allow the study objectives to be met and to best allow for the comparison of the freeze system variants. Further details on the rationale of the start-up sequence is provided in SRK memorandum, "Giant FOS – Start-Up Protocol" dated November 5, 2010 in Appendix C.

The objective in determining the start date for each group or freeze variant was to start them as early as possible—and concurrently where required—without compromising the ability to make direct comparisons between the freeze technology variants or any related components in the Remediation Plan, e.g., drift plugs.

Groups A, B, C and M on the east loop of Chamber 10 were activated upon start-up at the same time at the end of February 2011. This approach allowed for:

- Groups A and B to provide a direct comparison of active freezing between the active and hybrid thermosyphon technologies.
- Groups A and M to provide a direct comparison of active freezing with 4.5- and 3-inch sized piping.
- To have a fair comparison between Groups A and B, Group C was turned on at the same time as Group M. This was to show that boundary effects north of Group A are similar to boundary effects south of Group B.
- Groups F and G were operated as passive thermosyphons for the remaining winter and into spring of 2011. They were switched to hybrid mode on May 25, 2011 once air temperatures warmed to the extent that passive operation became ineffective. Operation of Groups E and H were delayed until the switching of Groups F and G to hybrid operation to avoid interference when operating in passive mode.
- Comparison of 4.0 inch thermosyphons versus 2.5 inch thermosyphons under both passive and hybrid operation
- Passive operation allows for a further understating of how the climate influences what is happening in the ground.

The decision to activate Groups D, J, K, and L will not be made until a plan for the drift plugs is finalized. If the selected drift plug design is such that the plugs will not be impacted by frozen conditions, the groups may be activated. Otherwise, these groups are to be activated following the plug installations.

The underground freeze pipes were activated in late February 2011 concurrently with the surface Groups A, B, C and M. Activating the underground pipes allowed for the potentially saturated dust in the bottom of the chamber to start freezing as soon as possible. The additional cooling load at the Startec freeze plant from the underground pipes, allowed it to operate within its optimum range.

4 Study Timeline

Figure 4-1 summarizes the study operations since the start of ground freezing on February 28, 2011, up to September 8, 2011.

Commissioning of the active and hybrid systems began in late February. The hybrid thermosyphons were charged during the last week of February, which marked the start of ground freezing. From March 2 to 9, the freeze plants were commissioned. During this time, all freeze Groups for both freeze systems were intermittently operated actively. This included thermosyphon Groups F and G where the refrigerant loops to the heat exchange coils had been shut off after commissioning to allow them to operate passively for the first three months of the study.

Following commissioning of the Dynalene freeze system (Dynalene is the heat transfer fluid circulated through the active freeze system), Groups A, C, M and the underground freeze pipes left in operation. Of the hybrid thermosyphon Groups, Group B was operated actively and Groups F and G were operated passively. From March 9 to April 19, AFCL operated Group B using only Coil A; Coil B was left switched off. The cold weather during this time enabled passive operation of the thermosyphons to assist the heat exchange coil in cooling the ground. On April 19, Coil B was activated, increasing the cooling power of Group B. From April 19 to 21, Groups F and G were also actively operated as a check to ensure the hybrid system would operate as intended.

On May 25, 2011, thermosyphon Groups F and G were switched from passive to active operation. Activation followed a period of warm weather where air temperatures were consistently above the measured pipe temperatures, indicating that no passive heat removal was occurring. The neighbouring Dynalene Groups, E and H, were also activated at this time. The flow rates through Groups E and H were gradually increased to the target rate of 3.5 m³/hr, from May 25 to June 9 to avoid a large increase in load at the Startec plant.

Groups D, J, K and L are in areas where drift plugs are to be installed underground. Activation of these Groups is dependent upon the design (by others) for drift plug installation.



Last Update: 23-Sep-11

DISO Calup: EW699-104118

Source File: FOS Operation Timeline.1CS019.018.pm.rev02.xlsx

Figure 4-1: FOS Operation Timeline

5 Performance Monitoring

The following sections outline the components of the study that are routinely monitored, how performance is assessed and the purpose of the data collection.

5.1 Monitoring of Ground Temperatures

Thirty-four dedicated instrumentation holes monitor ground temperatures throughout the study area (31 vertical holes drilled from surface and 3 horizontal holes drilled from the AR2 East Drift). Each hole contains a bundle instrument cable with 11 thermistor sensors. The vertical instrumentation holes are designated by the prefix “S” and their locations are provided in Figure 3-1. The figure also includes the sensor locations for the three horizontal holes, UG04, UG11 and UG16, located beneath Chamber 10. Further details of the thermistor locations are provided in SRK (2010a).

The ground temperature data is monitored regularly to track the progression of ground freezing and is also used for model calibration purposes to improve estimates of material properties, heat transfer efficiencies and freezing time predictions.

5.2 Climate Monitoring

The site climate has a direct impact on the thermal regime of rock near the surface, the thermosyphon performance and the performance of the freeze plants. The FOS weather station tracks the following climatic data on an hourly and daily basis:

- Average air temperature (°C)
- Average relative humidity (%)
- Average barometric pressure (kPa)
- Average wind speed (m/s)
- Average wind direction bearing and standard deviation (°)
- Maximum wind speed (m/s)

The temperature and wind data is required for calculations of passive heat flux for the hybrid thermosyphons detailed in Section 5.3.2.

5.3 Monitoring of Individual Freeze Pipes

The following sections list the parameters monitored for each individual pipe as well as the calculations used to derive the heat extraction rate. The parameters are monitored regularly to track trends and watch for unexpected changes that may affect freeze performance.

5.3.1 Active Freeze Pipes

At each active freeze pipe the Dynalene flow rate and the temperature as it enters and exits the pipe are measured. Measurement of these parameters allows the total heat flux, Q_{total} (kJ s^{-1}), to be calculated based on the formula:

$$Q_{\text{total}} = \dot{m}C_p\Delta T \quad (\text{Eq. 1})$$

where \dot{m} is the Dynalene mass flow rate (kg/s), C_p is the its mass heat capacity ($\text{kJ kg}^{-1} \text{ }^\circ\text{C}^{-1}$) and ΔT is the difference between the Dynalene supply and return temperatures at the freeze pipe. At -35°C , the density and mass heat capacity of Dynalene are $1,300 \text{ kg/m}^3$ and $2.8 \text{ kJ kg}^{-1} \text{ }^\circ\text{C}^{-1}$, respectively.

Six freeze pipes (P01, P08, P12, P14, P15 and P38) are instrumented with thermistor strings that measure pipe temperatures at up to 11 points along the pipe. The temperature measurements are used to estimate heat transfer coefficients that are in turn used to model the convective heat transfer between the cooling fluid and the outside of the freeze pipe.

Details of the heat transfer coefficient testing and results are provided in Section 8.1.6.

5.3.2 Hybrid Thermosyphons

For each hybrid thermosyphon, the following parameters are monitored:

- Mass flow rate of the liquid refrigerant through each coil measured inside the freeze plant
- Absolute pressure of the liquid refrigerant measured at the sub-cooler outlet header inside the freeze plant
- Absolute pressure of the vapour refrigerant entering the freeze plant (suction pressure)
- Refrigerant temperatures in and out of each coil
- Radiator (condenser) temperature above the coils
- Evaporator (pipe) temperature below the coils at the ground surface

Figure 5-1 provides a schematic diagram of a hybrid thermosyphon as well as the location of the temperature sensors. 9 of the 12 hybrid thermosyphons are also instrumented with thermistor strings to monitor pipe temperature at up to 11 points along the pipe. The thermistors are monitored to ensure that there is no "choking" of the circulation fluid (carbon dioxide) and there is cooling occurring along the full length of the pipe.

Active heat extraction rate by the refrigeration coils is calculated using pressure-enthalpy relationships of the refrigerant. The refrigerant fluid used in the thermosyphon exchange coils is R507. Energy extraction calculations are detailed in a memorandum prepared by Eascan Automation Inc., on behalf of AFCL, dated September 27, 2010 (Appendix C).

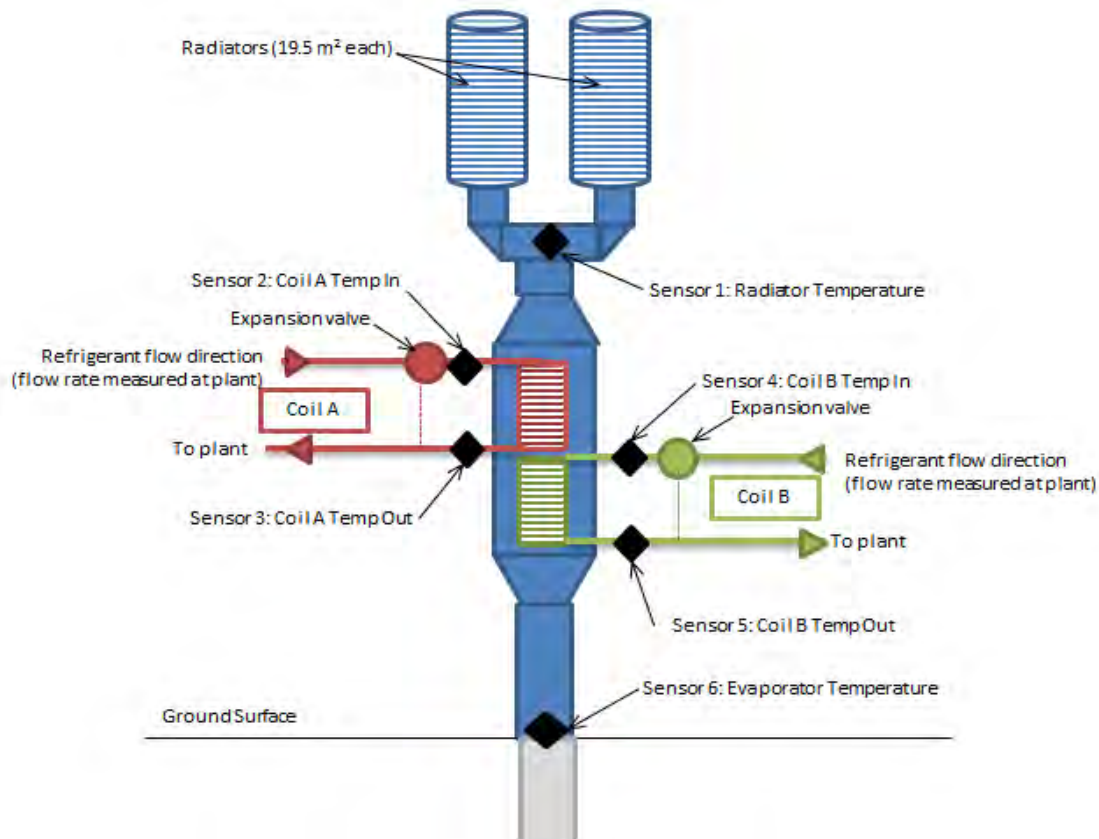
The passive heat extraction rate can be described by the following expressions:

$$Q = h (T_{\text{soil}} - T_{\text{air}}) \quad \text{for } T_{\text{air}} < T_{\text{soil}} \quad (\text{Eq. 2})$$

$$Q = 0 \quad \text{for } T_{\text{air}} > T_{\text{soil}} \quad (\text{Eq. 3})$$

$$h = (A + B V^C) A_{\text{rad}} \quad (\text{Eq. 4})$$

where Q is the total heat flux (J s^{-1}), h is the heat transfer coefficient ($\text{J s}^{-1} \text{ }^\circ\text{C}^{-1}$), T_{soil} is the temperature of the evaporator in the ground ($^\circ\text{C}$) (Sensor 6 in Figure 5-1) and T_{air} is the ambient air temperature ($^\circ\text{C}$). In Equation 4, V is wind speed (m/s), A_{rad} is the radiator surface area (m^2) and A , B , and C are fitting coefficients based on measurements.



Source File: Hybrid Thermosyphon Schematic.Figure.1CS019.018.pptx

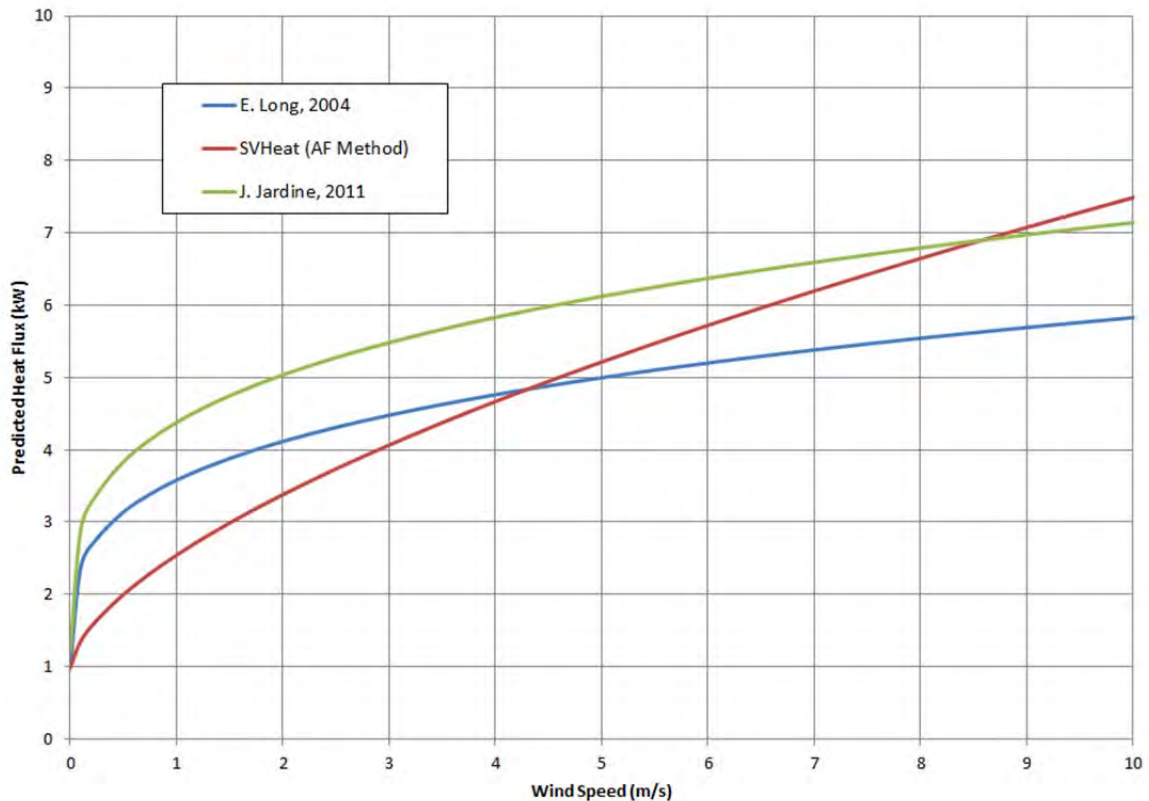
Figure 5-1: Hybrid Thermosyphon Schematic

Table 5-1 provides three sets of the heat transfer coefficient fitting parameters, all based on AFCI's sources. Set 1 was used during the conceptual design engineering reported in SRK (2006) and was provided by E. Long of Artic Foundations, Inc. (AFCI's counterpart in the United States) in 2004. Set 2 was obtained from the SVOOffice 2009 User's Manual (2009), where it is listed as the "Arctic Foundation's Method". Set 3 was obtained from personal communication with John Jardine of AFCI in February, 2011.

Figure 5-2 provides a comparison of the predicted heat flux for a range of wind speeds assuming air and ground temperatures of -10 °C and 0 °C respectively. The comparison also uses a total thermosyphon radiator surface area of 39 m², which is the same total area for the hybrid thermosyphons in Groups B, F, and G. Depending on the wind speed, there is a considerable difference in the predicted fluxes for each formula. An evaluation of the heat transfer coefficient formulas is provided in Section 8.3.

Table 5-1: Comparison of Thermosyphon Performance Coefficients

	Set 1 AFCI (E. Long), 2004	Set 2 SV Heat, 2009	Set 3 AFCI (J. Jardine), 2011
A ($\text{J s}^{-1} \text{C}^{-1}$)	2.59	2.52	2.72
B ($\text{J s}^{-1} \text{C}^{-1} (\text{m/s})^{-0.5}$)	6.58	4	7.04
C (unitless)	0.273	0.62	0.273



Source File: Thermosyphon Heat Flux Formula Comparison.xlsx

Figure 5-2: Thermosyphon Heat Flux Formula Comparison

5.4 Monitoring of Freeze Groups

Individual pipe fluxes, flow rates and temperatures are plotted by group to monitor for any change in relative performance and for any problems or changes in operation.

5.5 Monitoring of Distribution Loops

The Startec plant supplies chilled Dynalene for the active freezing system. The distribution piping outside the plant has three separate circuits, or loops, that distribute Dynalene to freeze pipes on the east side of the chamber, to the west side of the chamber and to the underground freeze pipes. Each loop has two parallel pipes, one for supply flow and the other for return flow. Each distribution loop is monitored constantly for flow rate, supply and return pressures for changes that could indicate a leak in the system or drift in flow control valve settings.

Resistance Temperature Detectors (RTD) were to be installed on each loop to monitor Dynalene temperatures prior to entering the plant. They were not installed before commissioning, but are expected to be installed and operating in November 2011. The sensors will be used to determine the heat gain between freeze pipe and plant to assess the overall efficiency of the system. Once the data becomes available, the historical temperatures for each distribution loop since start-up freezing are to be calculated.

5.6 Monitoring of Freeze Plant Performance

The efficiency of a freeze plant is measured by the Coefficient of Performance (COP). It is calculated as the ratio of ground heat extraction to the energy input into each freeze plant as shown in the equation:

$$\text{COP} = \frac{Q_{\text{total}}}{W_{\text{in}}} \quad (\text{Eq. 5})$$

where Q_{total} (kJ s^{-1}) is the rate of heat extraction rate and W_{in} (kJ s^{-1}) is the total energy usage for the plant (including ancillary loads, e.g., building heat, ventilation fans, lighting, etc.).

Two different heat extraction rates may be used in the calculation depending on the purpose. The sum of heat extracted at each pipe is used to determine the efficiency of ground heat extraction. To measure the efficiency of the overall system, including heat gains along the distribution loops, the parameters measured at the plant are used, e.g., overall Dynalene flow rate and Dynalene temperatures in and out of the plant.

Temperature sensors are yet to be installed on the return line on each distribution loops prior to the Dynalene returning to the plant. Installation of these sensors will allow the efficiency of each distribution loop to be determined.

The COP findings for both freeze plants are discussed in Section 8.1.5.

6 Data Management and Data Handling Methods

6.1 Data Management and Collection Frequency

The following sections briefly describe the Supervisory Control and Data Acquisition (SCADA) system for the project, and how the data is stored and processed for analysis. Further details on the SCADA system can be found in the AECOM and AFCI documentation.

There are five Programmable Logic Controller (PLC) computers for the FOS project that capture and process the instrumentation signals and record data.

- **Freeze Project PLC:** Located in the instrumentation building, the PLC monitors and controls the thermistor sensors, vibrating wire piezometers, freeze loop temperatures, flow rates, and pressures.
- **Weather Station PLC:** Also located in the instrumentation building, the PLC monitors and records data from the weather station installed outside the building.
- **Underground PLC:** Located in the AR2 East drift and enclosed in an instrumentation cabinet, the PLC monitors and controls the underground thermistors, freeze pipe temperatures and flow rates.
- **Startec Plant PLC:** Located in the Startec plant, the PLC monitors and controls the refrigeration equipment status, power consumption, coolant levels, flow rates and pressures, and refrigerant leak detection.
- **AFCI Plant PLC:** Located in the AFCI freeze plant, the PLC monitors and controls, the hybrid thermosyphon pipe temperatures, refrigerant flow rates and pressures, refrigeration equipment status, power consumption, coolant levels and refrigerant leak detection.

Programming of the AFCI plant PLC was completed by EASCAN Automation Inc. under subcontract to AFCI. Integration of all PLC's was conducted by AECOM.

Graphic displays at each PLC, except the weather station, provide real time and historical data charting. The PLC's log data at programmed intervals or based on exception rules. At this time, documentation of the exception rules has not been received by SRK. The AFCI plant PLC records data at five minute intervals and stores it on the PLC hard drive for a period of six months. For all other PLC's, most data is recorded at 20 minute intervals or if the value changes by a certain percentage. The following parameters are exceptions to the above rules:

- The weather data is recorded as hourly averaged data; and
- The Startec power consumption is recorded on a cumulative basis every three hours.

The PLC's are connected by fibre optic cable to servers located in the C-Dry building. The servers in C-Dry store the raw data, logs alarms and auto-dialer activity. Raw data is managed on site using FactoryTalk Historian System Management software produced by Rockwell Automation. Data compression is performed on the raw data at the historian. There, if a parameter does not change over the specified regular time interval, values will not be recorded—except for the first and last values during these periods that allow for interpolation between records at any time.

The servers in C-Dry are accessible off-site through the Internet. Data back-ups are regularly performed by both Public Works and SRK. SRK backs up the data daily in a SQL Server database

that allows flexible data access options for monitoring and analysis. The SRK memorandum entitled “Giant FOS – Data Management” dated Oct. 26, 2010 provided in Appendix C further details SRK’s decision process for data handling for the project.

Microsoft Excel is used as the front end user interface to perform calculations and track performance. Queries are first set up in the SQL Server that groups data into views (e.g., Group A data) and imports the data to an Excel spreadsheet. For most parameters that record multiple readings per hour, the queries also pre-process the data to provide values at regular matching time intervals for all parameters in the view (e.g., hourly, daily). This is done by rounding each time stamp to the nearest hour and then averaging the data. A common time stamp is required in order to complete the energy calculations.

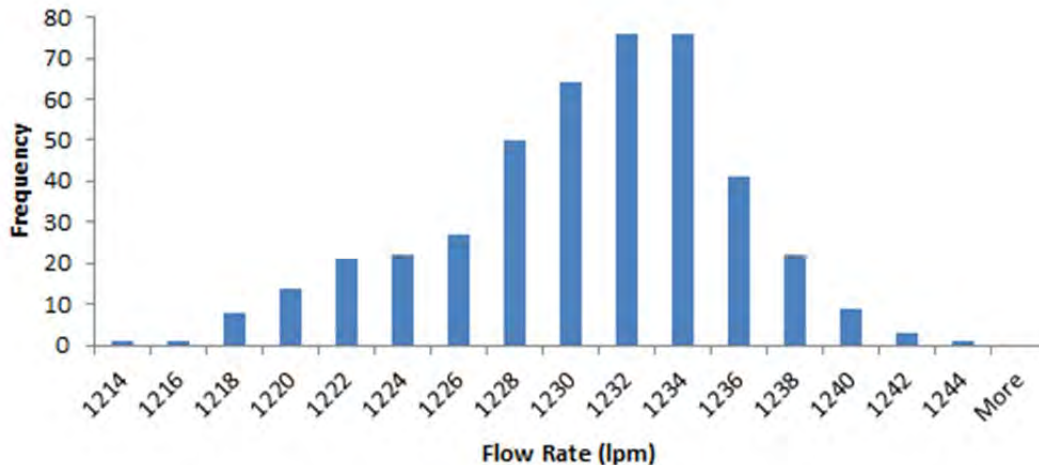
Parameters not pre-processed by the SQL queries consist of weather and power consumption data. Weather data on the historian server is already in an hourly (or daily) averaged format with common time stamps. Power data is logged on a daily and monthly cumulative basis in kWh units.

On May 9, 2011, an analysis was completed on the data collection frequency for all recorded instrumentation. A total record count to each distinct instrumentation tag was compiled over the first 72 days of operation. The record totals are from raw data, prior to any compression by the historian system. It was found that 63 distinct tags record data more than twice in an hour, while 8 of these tags recorded over 100 readings per hour. Table 6-1 lists the top six instrumentation tags in terms of recording frequency. The table groups together all ‘FIT’ tags (hybrid thermosyphon flow meters), as they all have a high recording frequency. At least 4 FIT tags record over 100 readings per hour.

Table 6-1: Data Collection Frequency Rankings – Up to May 9, 2011

Rank	Instrumentation Tag	Avg. Records per hour	Description
1	Startec_PLC.FE_500	385	Dynalene Supply Flow Rate
2	PT_M01_041	297	East Loop Dynalene Pressure Supply
3	FIT#,#	Max: 214 (FIT1,1) Average: 70 Min: 14 (FIT1,12)	Hybrid Thermosyphon flow meters
4	FT_M01_041	140	East Loop Dynalene flow rate
5	FCV_M01_021.SCADA.ZI	103	Underground Loop Dynalene Flow Rate
6	PLC.PT_150	39	Startec plant compressor discharge pressure – NH ₃ loop

Figure 6-1 provides a histogram that illustrates the variability in the Dynalene supply flow rate (tag: Startec_PLC.FE_500). The histogram was completed to determine if the high record count is due to high variability or if the exception rule is set too small. The histogram includes 436 records over a period of 1 hour. Flow rates during this period ranged from 1,213 lpm to 1,243 lpm, with a median value of 1,230 lpm. The minimum and maximum differ from the median by 1.4% and 1.0% respectively. In this case, the exception rule should be increased to reduce the quantity of data collected. The list of collection frequencies was provided to AECOM for review of the exception rules. It is not known if any changes were made.



Source File: DistinctTagandRecordsCounts.1CS019.018.pm.xlsx

Figure 6-1: Startec_PLC.FE_500 Data Collection Histogram

6.2 Data Collection Issues and Recommendations

This section presents the data collection issues encountered during operation of the FOS, with regards to handling of the data for analysis. Issues and reliability of the instrumentation hardware is discussed in Section 8.8.

1. **Network Issues:** No data was collected during May 24 to 26, 2011. An error occurred on the Historian Server on May 24 that resulted in a stall on the interface between the historian and SCADA servers. The servers were rebooted and logging resumed. All data during this period was lost, except for the weather station data that was manually collected at the time.
2. **Historian Data Compression:** As mentioned above, the historian compresses data on the server where readings do not change. For example, the compression is common for refrigerant pressures and temperatures from the AFCI plant which are required for heat flux calculations. Data is generally recorded every 2 to 4 hours with no common time stamp frequency among all the parameters needed to complete the energy calculation. To complete the calculations, hourly averaged data is first imported into Excel. If no data exists in a certain hour, it is assigned the average of the previous hour's value. This procedure introduces a bias into the analysis; more accurately, the value should be equal to the last recorded value and not the previous hourly average. Generally, the variation is small. Comparisons to the heat flux using raw data have shown that the difference is insignificant.
3. **Recording Errors and Skipped Data:** There have been instances where data is skipped and not recorded, or records with odd characters become part of the data set. The cause of the 'hiccups' in the system is not known at this time. Examples of these hiccups are:
 - On May 9, 13:16, six records of the PT_M01_041 tag (east loop Dynalene pressure) had odd characters inserted. These are shown in Figure 6-2. The first and last lines of the data set are normal records. The records were manually deleted from the SRK SQL Server.

```

2011-05-09 13:16:42.277000000|MainPLC.PT_M01_041.HIST|98.563820000000007|0
2011-05-09 13:16:44.277000000|MainPLC.PT_M01_041/HIST|903.4901|0
2011-05-09 13:16:45.277000000|MainPLC.PT_M01_041>HISTDC4|97.239677|0
2011-05-09 13:16:47.277000000|MainPLC.PDC4_M01_041.(IST|107.425389999999999|0
2011-05-09 13:16:48.293000000|MainPLCnPT_M01_041.HIST|97.1378169|9 9998|0
2011-05-09 13:16:51.293000000|MainPLC.PT_M01_041.HIST|18801384|0
2011-05-09 13:16:52.277000000|MainPLC.PT_M01_041.HIST|99.752150999999998|0
2011-05-09 13816:56.293000000|MainPLC.PT_M01_061.HIST|106.370830000000001|0
2011-05-09 13:16:57.293000000|MainPLC.PT_M01_041.HIST|95.100669999999994|0

```

Source File: GiantFOS_OpWeeklyReport 08.20110513.doc

Figure 6-2: Data Collection Error Example – PT_M01_041, May 9, 2011

- On August 2, 2011, at 16:00 a hiccup occurred in the weather station data set. Since this time, air temperature and other parameters record data every one to three hours. Restoration of an hourly collection frequency is currently under investigation by AECOM.
4. **Startec Plant Cumulative Power Consumption:** Cumulative power consumption is tracked for the Startec plant on a daily and monthly basis. The PLC is programmed to record the maximum consumption at the end of the day before the counter is reset. The data is used in the Coefficient of Performance (COP) calculations described in Section 8.1.5. In the COP calculation, a query returns the maximum kWh for each day, and the daily COP is calculated.

The issue that has arisen, is that the time stamp for the maximum power reading is not exactly at the end of the day (23:59:59), and will frequently occur on the next day, e.g., 00:00:04. In these cases, the maximum value returned by the query will be the preceding value that sometimes occurs up to three hours prior. This issue has been mitigated by subtracting the month-to-date totals for each day and requires a manual input of the days total for the last day of each month.

Summary of Data Management Recommendations

Based on the issues encountered in the data collection and management of the FOS to date, the following recommendations are made for the future freeze program:

- No data compression should be performed on the raw data.
- A common time interval should be established for all parameters that are required in the same calculation eliminate interpolation between data points.
- Instantaneous power consumption data should be tracked, as it used for the AFCI plant.
- Exception rules should be periodically reviewed and adjusted to reduce the overall quantity of data collected. The first review should be completed within the first couple of weeks following the start of operations. Subsequent reviews may be completed every six months thereafter.

7 Ground Freeze Progress to September 2011

Figure 7-1 provides an illustration of the approximate freeze progress to September 8, 2011, after approximately six months following the start of ground freezing operations. The figure is a 2D plan model section at an elevation of 125 m that is located approximately mid-height of the chamber. Temperature contours are plotted at 5 °C intervals. Details of the model simulation are provided in Section 8.1.2. The model used typical bedrock properties of 400 kJ m⁻¹ day⁻¹ °C⁻¹ and 2,425 kJ m⁻³ °C⁻¹. Daily averaged pipe temperatures were specified for each pipe.

Modeled temperatures at the instrumentation holes in bedrock were compared to recorded temperatures. The median deviation is 0.5 °C with a maximum deviation of 2.3 °C at S07 near Group C. The second highest deviation of 1.4 °C is located at S11 (Group F). In both of these cases, the recorded values are warmer than the temperature predicted by the model. The deviations do not significantly impact the temperature contours in Figure 7-1.

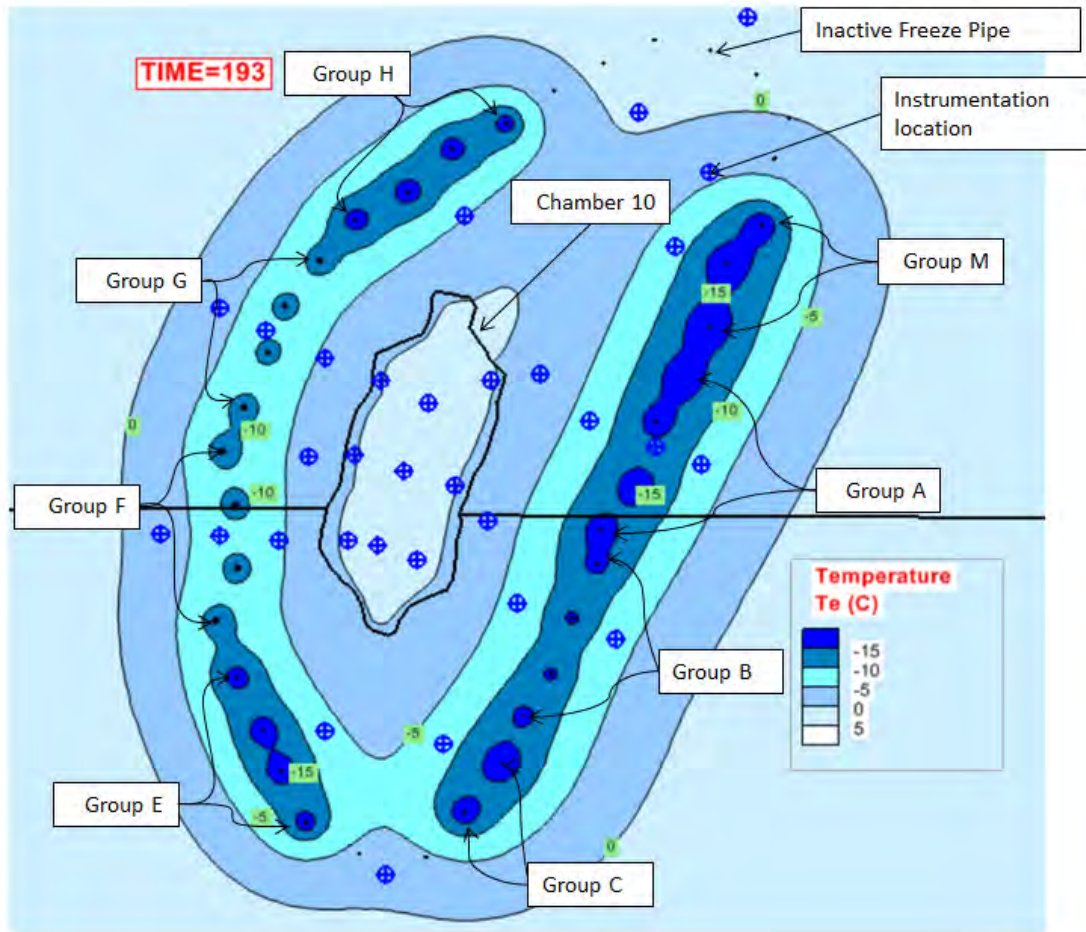
The ground freezing for the active freeze pipes has progressed further than anticipated to date compared to the conceptual design. Even without the activation of freeze pipes at the northern end southern end of the study, the 0 °C isotherm has surrounded the chamber on all sides.

Table 7-1 lists the approximate freeze wall thickness for the -5 and -10 °C isotherms for each operating group, measured at the thinnest point within each group.

Figure 7-2 provides the temperature profiles for the three thermistor strings installed parallel to the underground freeze pipes. Also noted on the graphs are nearby vertical freeze pipes. The temperature contour plot presented in Figure 7-1 is also overlain on the plot of underground freeze pipes. This provides context of the influence of the vertical freeze pipes on the east side of the Chamber on the horizontal freeze wall temperature profile.

There are very few thermistor sensors located to either side of the horizontal freeze pipe alignment. As a result, it is difficult to accurately estimate the freeze thickness for the group. The temperature profiles in Figure 7-2 show that along the alignment, the typical temperature between the pipes that is outside of the influence of the vertical freeze pipes is -15 °C. Compared to the plot in Figure 7-1, the typical temperature is similar to that found in Groups A and M. The wall thickness for the underground group is therefore expected to have a similar thickness.

Appendix B provides a series of photographs from the AR2 East Drift showing the freeze progress on the drift walls and the build-up of frost on the freeze pipes. On March 10, 2011, a small bedrock slab was dislodged from the wall of the second-level drift near Bulkhead #58 exposing freeze pipe P10. No other cracks or instability has been observed in the rock underground.

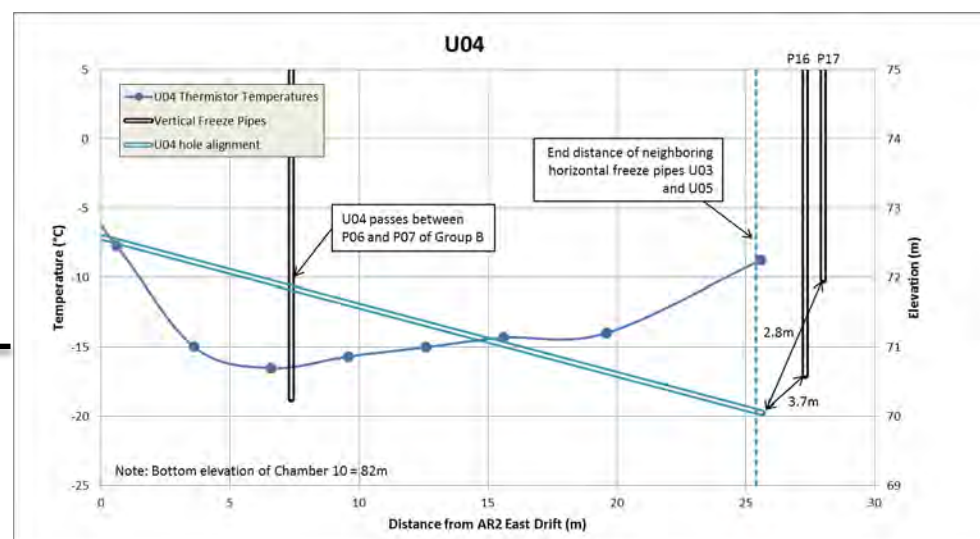
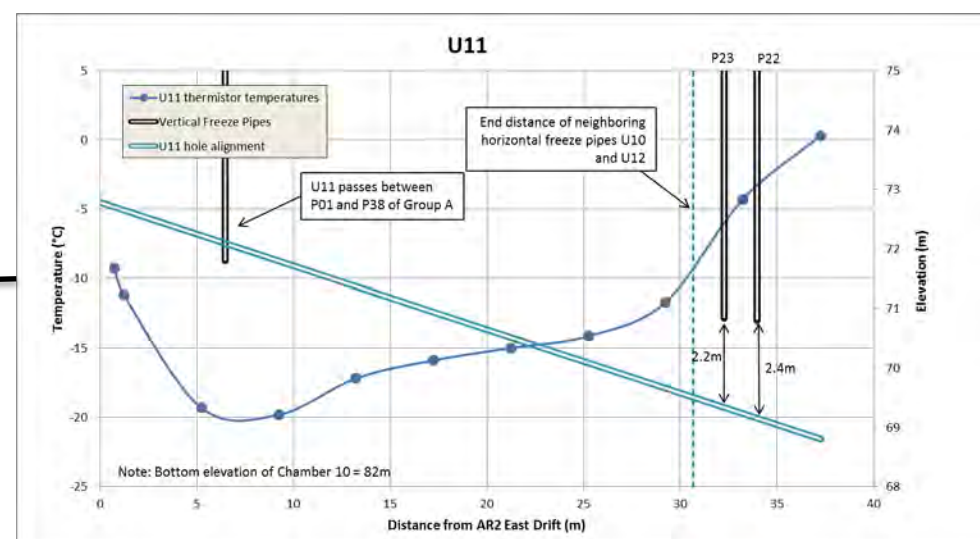
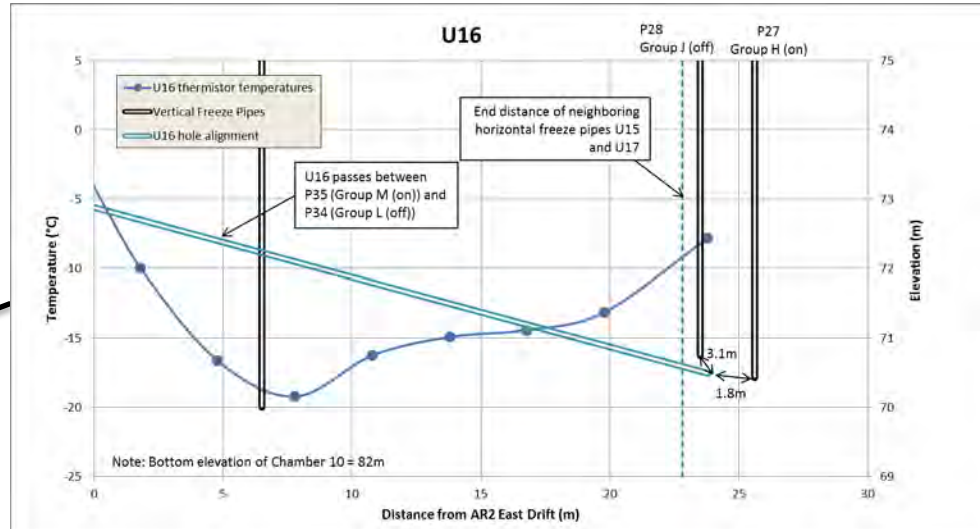
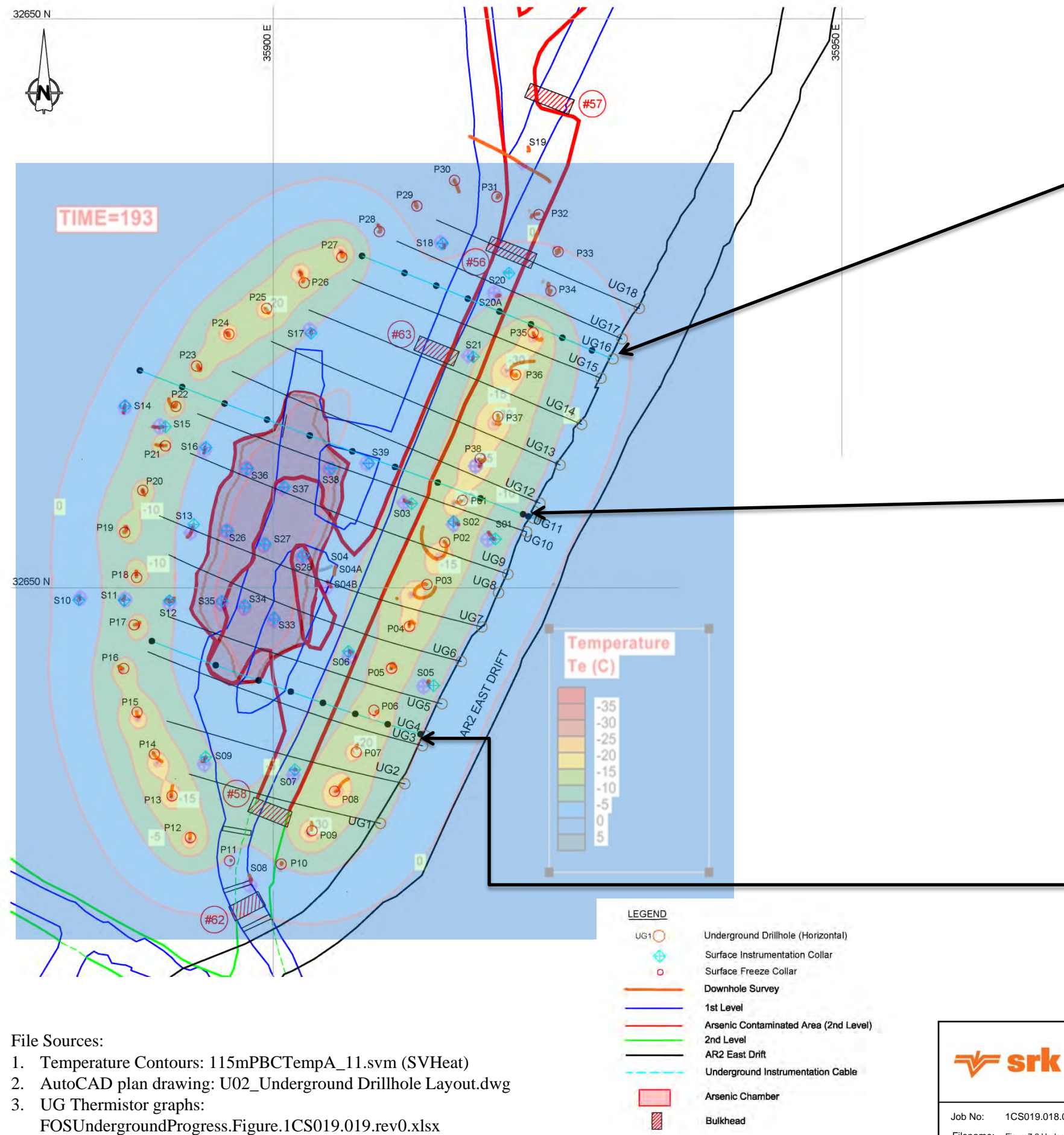


Source File: FreezeProgressSept8.Figure.1CS019.018.rev00.pm.pptx

Figure 7-1: Freeze progress up to September 8, 2011.

Table 7-1: September 8, 2011 Freeze Wall Thickness by Group

Group	Period of Operation	-5°C Wall Thickness	-10°C Wall Thickness
A	Active since March 7	11 m	5 m
B	Active since March 2	9 m	3 m
C	Active since March 7	10 m	5 m
E	Active since May 27	8 m	4 m
F	Passive: March 5 to May 25; Active: Since May 25	7 m	0 m
G	Passive: March 5 to May 25; Active: Since May 25	6 m	0 m
H	Active since May 27	8 m	3 m
M	Active since March 2	11 m	6 m



File Sources:

1. Temperature Contours: 115mPBCTempA_11.svm (SVHeat)
2. AutoCAD plan drawing: U02_Underground Drillhole Layout.dwg
3. UG Thermistor graphs: FOSUndergroundProgress.Figure.1CS019.019.rev0.xlsx



Job No: 1CS019.018.001
Filename: Figure7.2.UndergroundProgressSept8.1CS019.018.pm.pptx



Giant Mine

Freeze Optimization Study

Underground Freeze Progress up to September 8, 2011

Date: Sept 16, 2011
Approved: PHM
Figure: 7.2

8 Study Evaluation

8.1 Estimation of Parameters Needed for Design

8.1.1 Bedrock Thermal Conductivity

In the spring of 2011, the recovered drill core from the FOS construction was re-examined by SRK to obtain a better understanding of the mineralogy within the study region. The focus of the investigation was to obtain better estimates of the thermal conductivity based on the mineralogy near freeze Groups A, B, F and G. These groups were considered to be the main freeze technology variants evaluated in the study.

To make a fair comparison among these groups, differences in the bedrock properties near each group, which can affect the rate of freezing, needed to be taken into consideration. Figure 8-1 provides a plan of the study area with an examination of drillhole lithology and estimates of bedrock thermal conductivity based on the mineralogy. Eleven drill core samples were collected as representative of the range of bedrock types encountered. Thin sections of each sample were prepared and were analyzed under microscope by SRK to obtain the estimates of their mineralogical composition and orientation. Further details of the drill core investigation and mineralogical analysis are provided in Appendix A.

Table 8-1 provides the results of the mineralogical investigation along with the resulting estimates of thermal conductivity for each sample are summarized in Table 8-2. Thermal conductivities for each mineral were obtained from Clauser and Huenges (1995), and the thermal conductivity for the sample was estimated as the weighted geometric mean based on the mineralogical composition. For some minerals, a range of conductivities was reported in Clauser and Huenges (1995), depending on the method and orientation of the testing to the mineral axis. The ranges are noted in Table 8-2.

Table 8-1: Bedrock Sample Mineralogical Composition

#	Description	actinolite	chlorite	epidote	quartz	albite	sericite	titanite	calcite	opaques	biotite
11001	Basalt	40%	10%	10%	7.5%	2.5%	30%				
11002	Gabbro	48%				50%		2%			
11003	Pillow Basalt		40%	35%	15%		10%				
11004	Foliated Basalt/Gabbro		40%		15%	15%		8%	20%	2%	
11005	Basalt	30%	30%		10%	5%	15%	10%			
11006	Rhyolite	10%			75%					5%	10%
11007	Brecciated Basalt	6%	18%	4%	39%	6%	24%		3%		
11008	Pillow Basalt		35%		5%		25%		35%		
11009	Basalt		50%		20%			10%	20%		
11010	Pillow Basalt	40%		2%	5%	30%	20%	3%			
11011	Basalt/Gabbro	55%		2%	1%		40%	2%		<1%	

Source File: BedrockThermalConductivity.1CS019.018.rev01.KYK_ksk.xlsx

Table 8-2: Bedrock Sample Thermal Conductivities

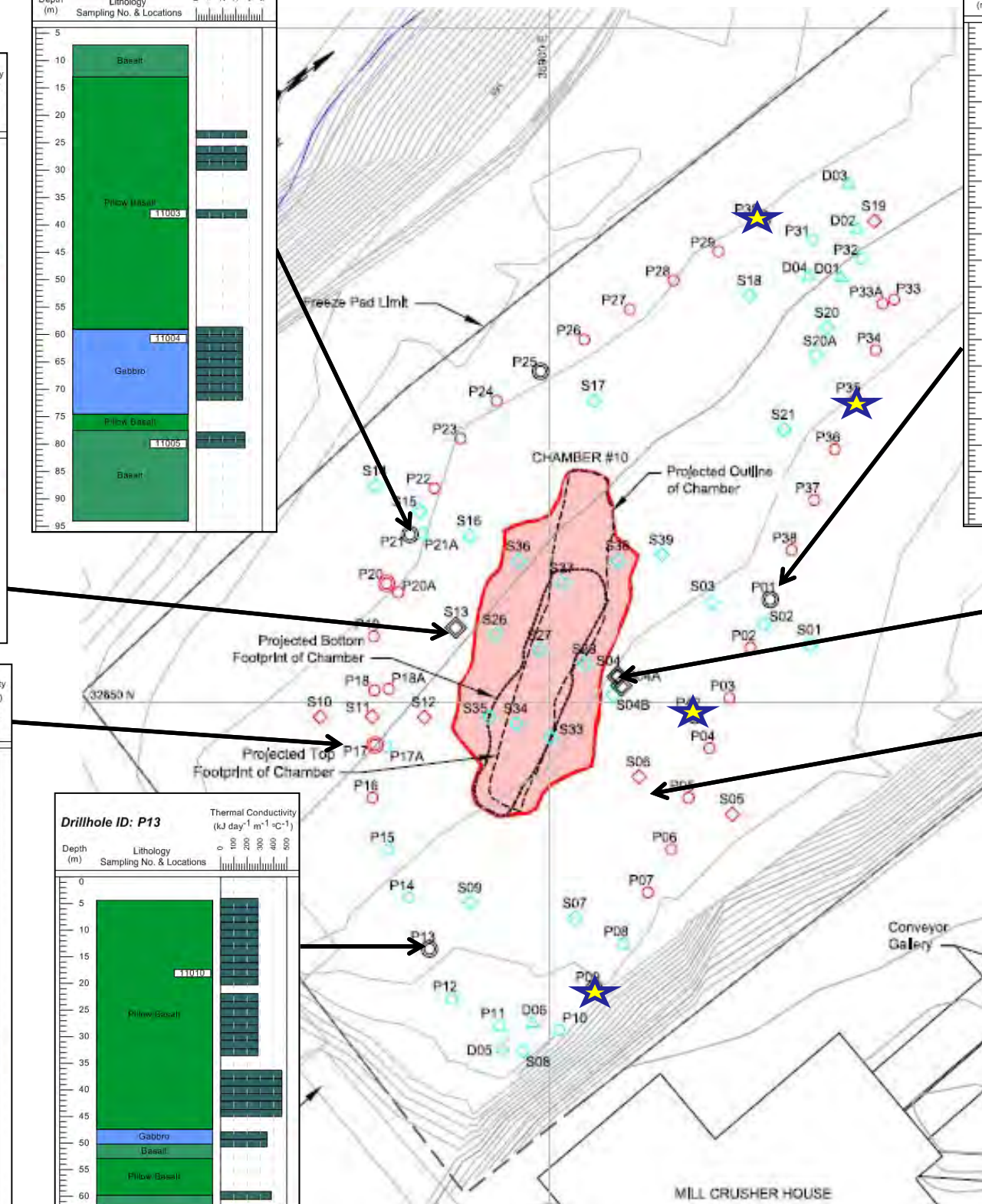
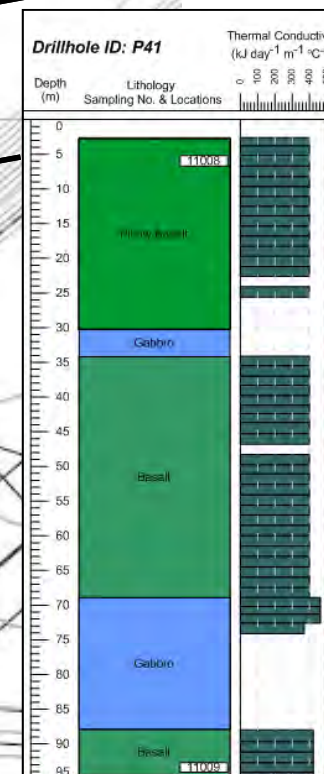
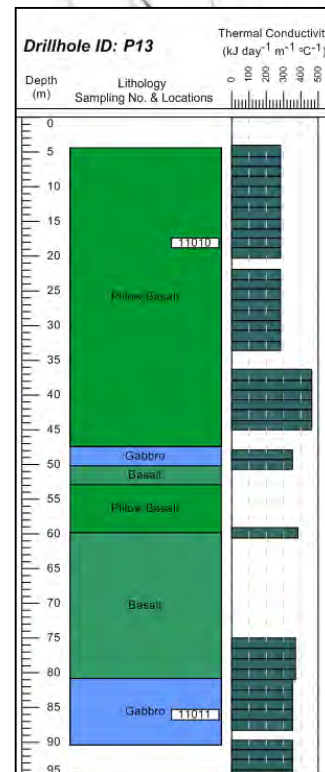
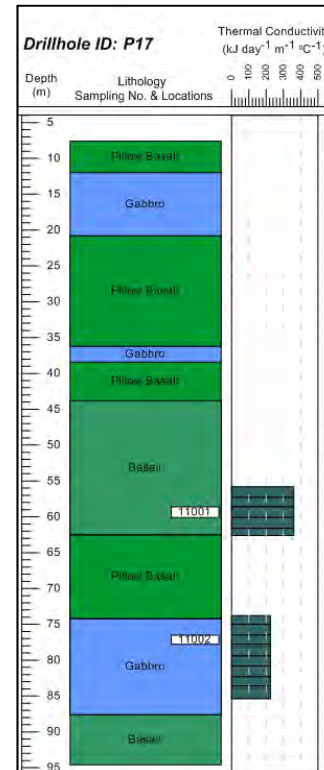
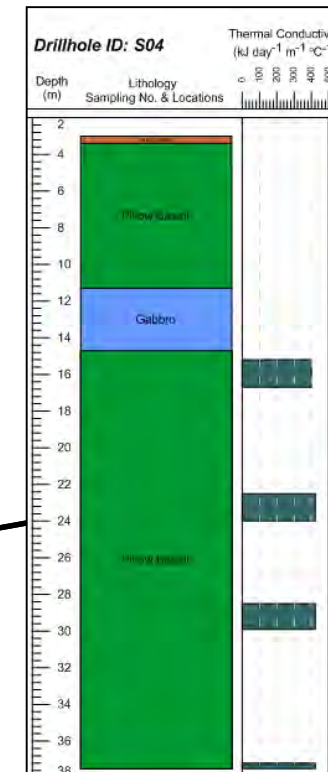
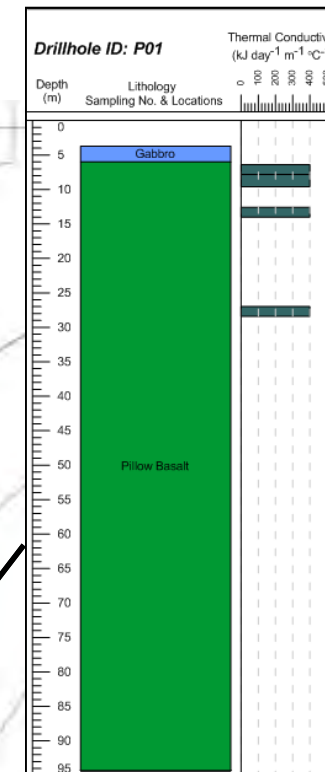
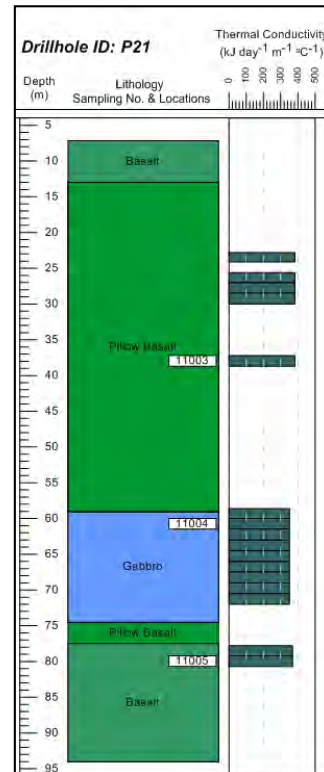
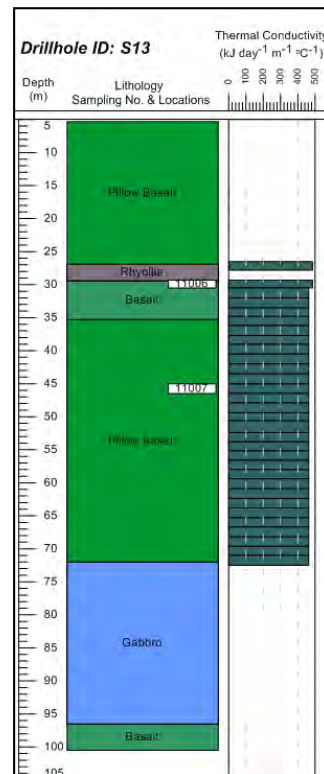
#	Drillhole	Depth Interval (m)		Description	Thermal Conductivity ($\text{kJ m}^{-1} \text{day}^{-1} \text{ }^{\circ}\text{C}^{-1}$)	Low Range Thermal Conductivity ($\text{kJ m}^{-1} \text{day}^{-1} \text{ }^{\circ}\text{C}^{-1}$)	High Range Thermal Conductivity ($\text{kJ m}^{-1} \text{day}^{-1} \text{ }^{\circ}\text{C}^{-1}$)
		From	To				
11001	P17	59.3	59.4	Basalt	361	317	377
11002	P17	76.5	76.7	Gabbro	234	226	245
11003	P21	38.3	38.4	Pillow Basalt	383	263	422
11004	P21	61.2	31.3	Foliated Basalt/Gabbro	350	222	405
11005	P21	80.6	80.7	Basalt	364	285	382
11006	S13	29.2	29.4	Rhyolite	485	225	676
11007	S13	45	45.1	Brecciated Basalt	466	297	553
11008	P41	5.9	6	Pillow Basalt	400	263	461
11009	P41	93.7	93.85	Basalt	415	242	483
11010	P13	17.4	17.5	Pillow Basalt	289	270	303
11011	P13	85.3	85.4	Basalt/Gabbro	350	346	352

Source File: BedrockThermalConductivity.1CS019.018.rev01.KYK_ksk.xlsx

Note: Higher thermal conductivity is a measure of how well a material can transfer heat: the higher the thermal conductivity, the faster heat is transferred.

The resulting estimates indicate that the thermal conductivity is expected to be uniform on the east side of Chamber 10 at $400 \text{ kJ m}^{-1} \text{day}^{-1} \text{ }^{\circ}\text{C}^{-1}$. However, the thermal conductivity was more variable west of Chamber 10, ranging from 230 to $485 \text{ kJ m}^{-1} \text{day}^{-1} \text{ }^{\circ}\text{C}^{-1}$. For comparison, the thermal conductivity used for thermal modelling in the Remediation Plan was $300 \text{ kJ m}^{-1} \text{day}^{-1} \text{ }^{\circ}\text{C}^{-1}$.

For modelling purposes described elsewhere in this report, a typical thermal conductivity of $400 \text{ kJ m}^{-1} \text{day}^{-1} \text{ }^{\circ}\text{C}^{-1}$ was used.



★ Other core recovery holes

8.1.2 Bedrock Thermal Diffusivity

A sensitivity analysis was completed to estimate the potential range of thermal diffusivity of the bedrock. Thermal diffusivity is the ratio of a material's thermal conductivity to its volumetric heat capacity and is expressed in units of m^2/day . The rate of modeled heat flow through a material can increase in two ways: increasing the thermal conductivity or decreasing the heat capacity. The use of thermal diffusivity in heating calculations reflects all possible combinations of those effects and is therefore used in the thermal modeling. The following sections describe the thermal model setup and results of the sensitivity analysis.

Sensitivity Model Setup

The sensitivity analysis simulated a 2D plan section located at approximately mid-chamber (elevation 115m, ~50m below ground surface). The model SVHeat Version 6, developed by SoilVision Systems Ltd., was used.

The 2D model plan geometry of the chamber at an elevation of 115 m was created from the GEMCOM underground model of the Giant Mine. This included the as-built locations of the drill holes for the freeze pipes and thermistor strings.

The bedrock and arsenic material properties used as the base case model are included in Table 8-3. Additional property details can be found in SRK (2006).

Table 8-3: Arsenic and Bedrock Physical Properties

Parameter	Arsenic	Bedrock	Units
Bulk Dry Density, ρ_{dry}	1345		kg m^{-3}
Specific gravity, G_s	3.38		-
Porosity, n	0.6	0.01	-
Volumetric water content, vwc	0.05	0.005	m^3/m^3
Thermal conductivity, k			
Dry unfrozen and frozen	8.0 and 17.3	300	$\text{kJ m}^{-1} \text{day}^{-1} {}^{\circ}\text{C}^{-1}$
Saturated unfrozen	81.2	300	
Saturated frozen	163.3	300	
Gravimetric heat capacity, c_g			
Dry unfrozen and frozen	0.6	0.81	$\text{kJ kg}^{-1} {}^{\circ}\text{C}^{-1}$
Saturated unfrozen	1.71	0.81	
Saturated frozen	1.06	0.81	
Volumetric heat capacity, c_v			
Dry unfrozen and frozen	807	2386	$\text{kJ m}^{-3} {}^{\circ}\text{C}^{-1}$
Saturated unfrozen	3327	2386	
Saturated frozen	2062	2386	

The first 127 days of freezing were simulated, running from February 28 to July 5, 2011. The initial temperatures were obtained from a steady state model simulation based on thermistor readings from February 28.

Averaged measured-averaged daily pipe temperatures, where available, were used as model input parameters to simulate each freeze pipe. The following assumptions were used to assign temperatures to un-instrumented freeze pipes:

- Groups D, J, K and L were not in operation except during commissioning were excluded from the model.
- In groups with some instrumented pipes (Groups B, C, E, F and G), average pipe temperatures from within the group were applied to the un-instrumented pipes.
- Group A consists of four active freeze pipes arranged in two parallel series of two pipes each. One series is instrumented (P38 and P01), while the other two pipes are not (P02 and P03). For modeling purposes the un-instrumented pipe temperatures were assumed to be the same for the first pipes in the series and also for the second pipes in the series. The temperature readings at P38 were assigned to P02, and similarly, temperatures at P01 were assigned to P03.
- Group H has no instrumented pipes, but has the same configuration as Group E, and was also activated at approximately the same time. The average pipe temperature values for Group E were applied to each Group H pipe.

The sensitivity analysis was completed prior to the revised thermal conductivity results being available. The analysis was performed with a fixed the volumetric heat capacity at $2,386 \text{ kJ m}^{-3} \text{ }^{\circ}\text{C}^{-1}$, the value listed in Table 8-3, and varied the thermal conductivity only. For the initial modeling, bedrock properties were assumed to be the same throughout the entire Chamber 10 domain. Additional modeling was later completed using the revised typical thermal conductivity of $400 \text{ kJ m}^{-1} \text{ day}^{-1} \text{ }^{\circ}\text{C}^{-1}$ to confirm the same sensitivity results would be achieved.

Thermal Diffusivity Sensitivity Results

The temperatures predicted by the model were compared to those measured in the ground by the temperature monitoring instrumentation. The base case model, using material properties used during the conceptual design, predicted temperatures around the freeze pipes that were generally higher than the measured temperatures, i.e., the rock was cooling faster than predicted by the base case model.

Figure 8-2 provides a plan view of the FOS area and indicates the thermal diffusivity that resulted in the best agreement between modelled and measured temperatures. Holes S08, S18, and S19 were excluded from the analysis because there was no significant temperature change to date. The typical diffusivity range and extreme values are provided in Table 8-4. Figure 8-3 provides time series graphs comparing the best-fit temperature responses to measured values for Groups A, B, F, and G.

Table 8-4: Estimated Range of Bedrock Thermal Diffusivity

Minimum Diffusivity (m^2/day)	Typical Diffusivity Range (m^2/day)	Maximum Diffusivity (m^2/day)
0.11	0.15 – 0.19	0.20

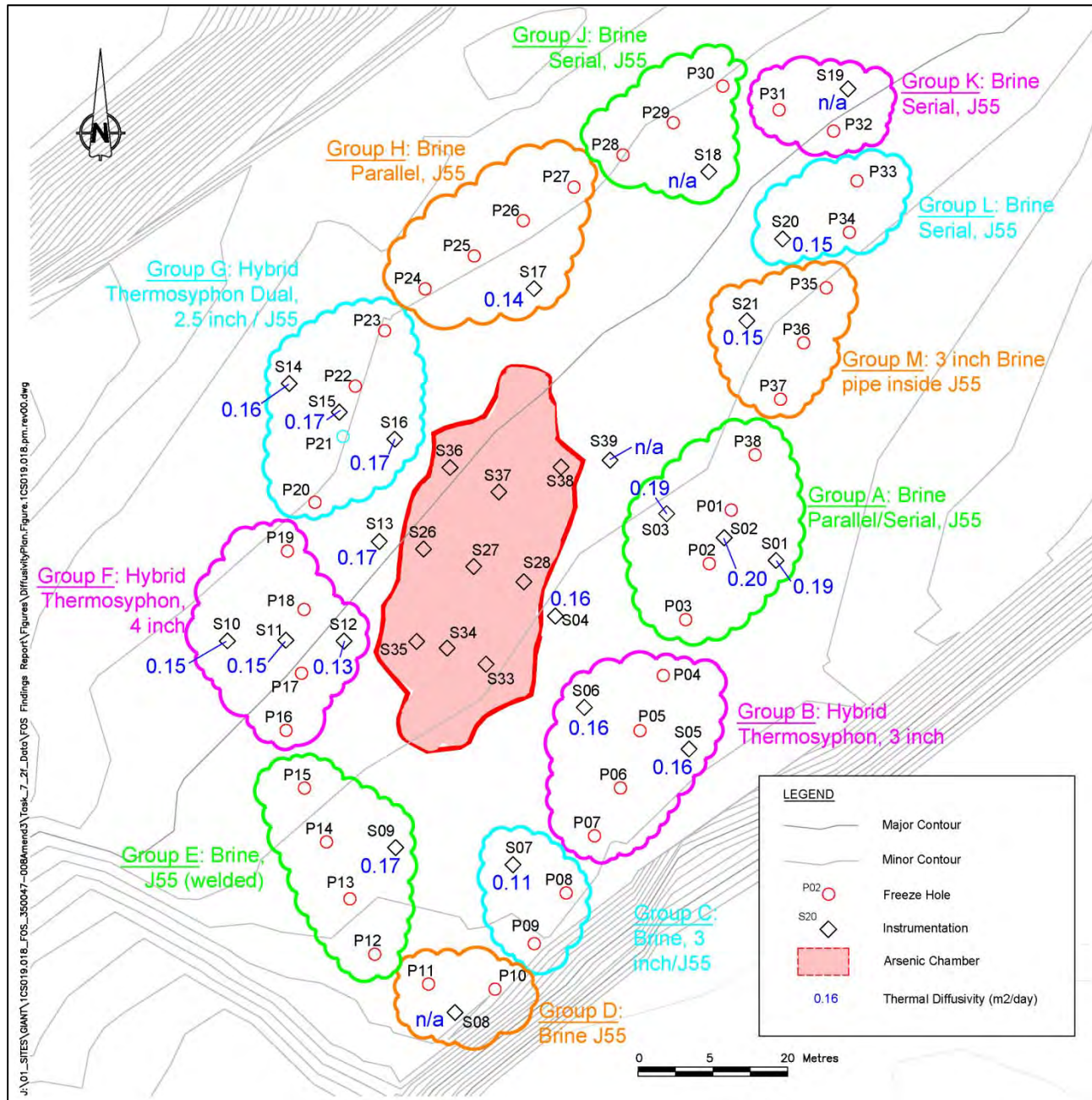
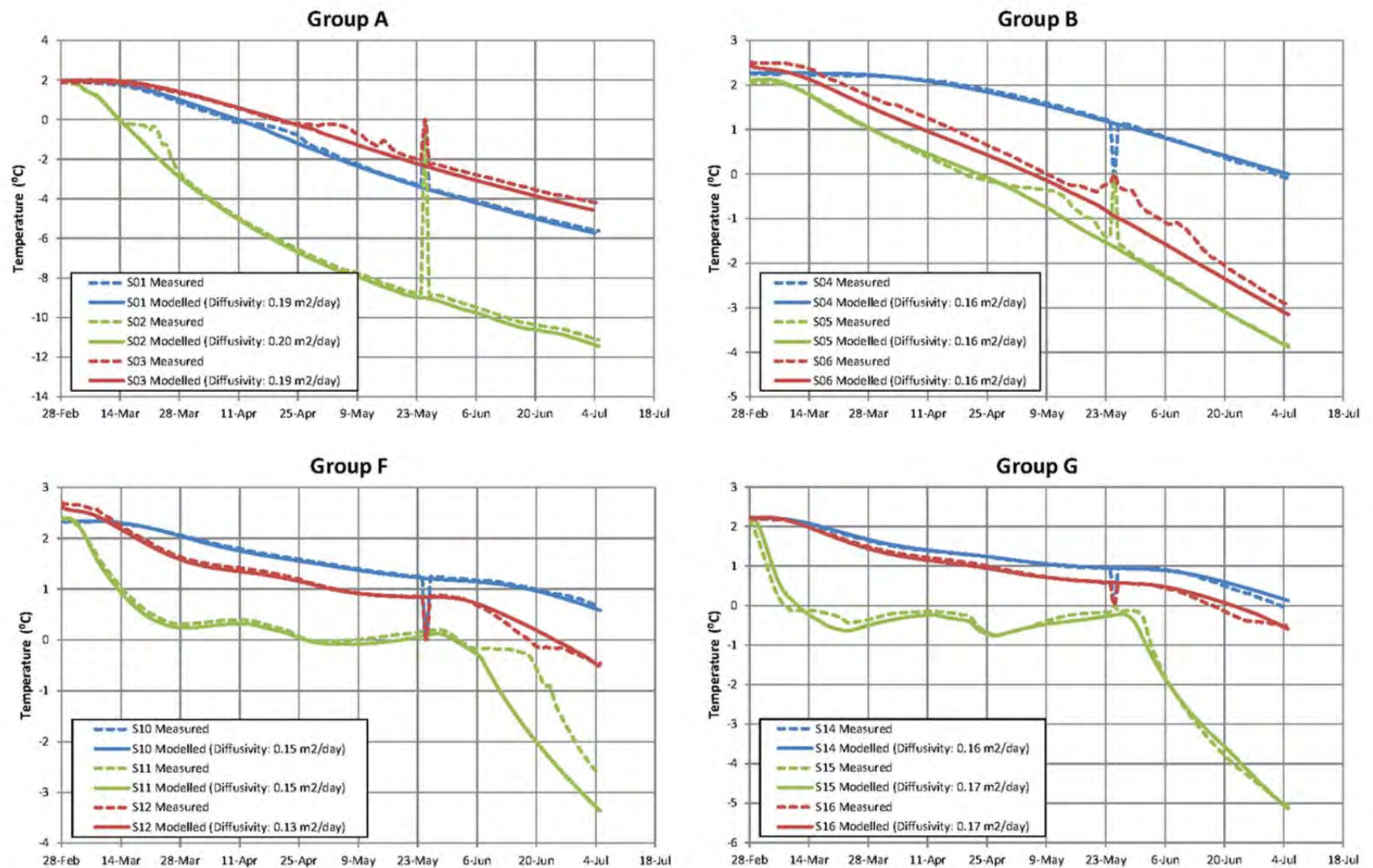


Figure 8-2: Comparison of Modeled Temperature Responses for Groups A, B, F and G



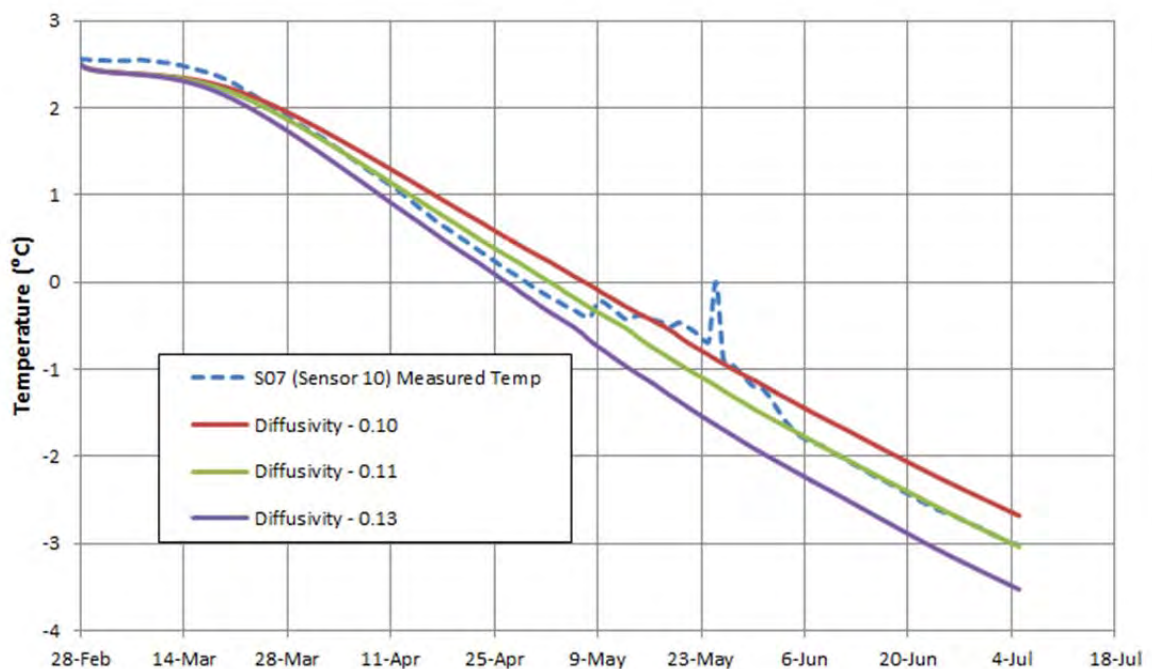
Source File: PMFigures.FOSFindings.1CS019.018.rev00.xlsx

Figure 8-3: Bedrock Diffusivity Model Calibration Results

The minimum diffusivity was observed at thermistor S07, offset four m inside the line of freeze pipes from Group C. S07 is located near S09 where the results of the drill core analysis found the lowest thermal conductivities.

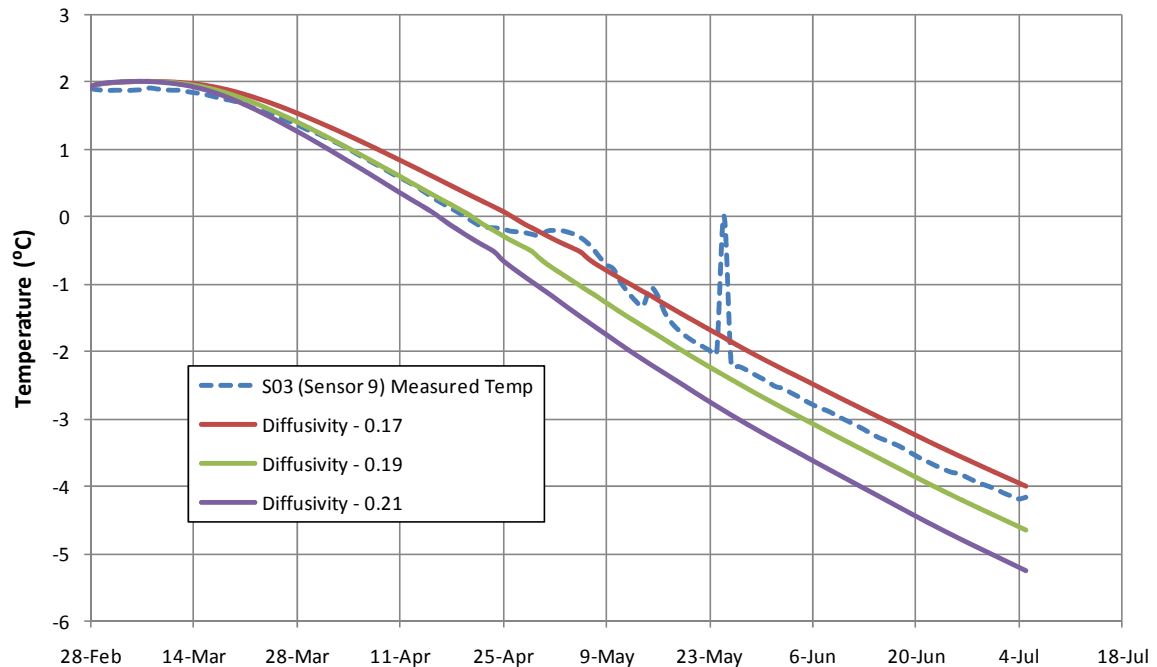
Another possible explanation for the slower cooling is the presence of geological structures that would obstruct heat flow. Figure 8-4 plots the actual and modeled temperature response at S07 for thermal diffusivities of 0.10, 0.11, and 0.13 m²/day. Results indicate a likely minimum thermal diffusivity of 0.11 m²/day, which is the best fit in Figure 8-4.

Temperatures measured at S02 indicated one of the quickest rates of cooling. Figure 8-5 compares the observed temperatures to model predictions using thermal diffusivities of 0.17, 0.19, and 0.21 m²/day. The results indicate a maximum thermal diffusivity of 0.18 m²/day.



Source File: PMFigures.FOSFindings.1CS019.018.rev00.xlsx

Figure 8-4: Modeled Temperature Responses at S07 for Various Bedrock Thermal Diffusivities



Source File: PMFigures.FOSFindings.1CS019.018.rev00.xlsx

Figure 8-5: Modeled Temperature Responses at S03 for Various Bedrock Thermal Diffusivities

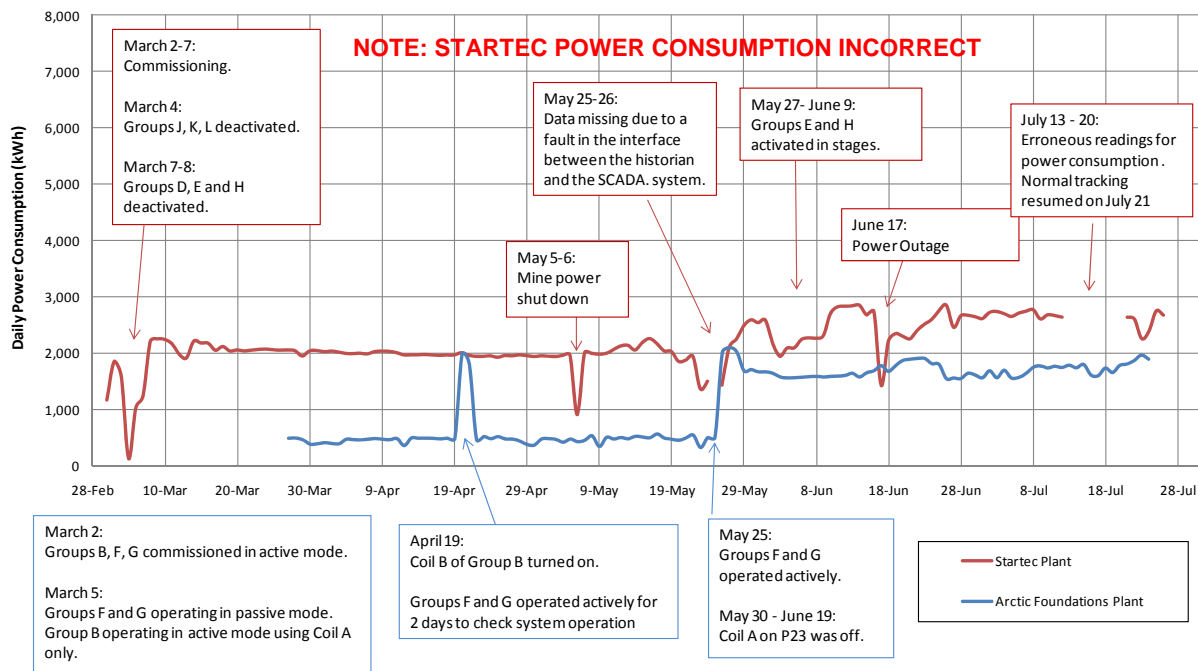
8.1.3 Arsenic Thermal Conductivity

As of the end of August 2011, the thermal properties of the arsenic cannot be calibrated with a thermal model as instrumentation had not detected the advance of ground freezing into the chamber.

8.1.4 Power Requirements

Figure 8-6 details the power consumption recorded for both the APCI and Startec freeze plants from the start of freezing at the end of February 2011 to the end of July 2011. Also noted in the figure are the major changes in the status of the freeze groups, power outages and instances of missing data.

NOTE: In mid-September discrepancies were found between the power meter at the Startec plant and the power consumption recorded by the PLC. The power meters have a "totalizer" that emits a pulse every 10 kWh's, and the PLC counts the pulses. It appears that not all pulses are being counted by the PLC. As a result the power consumption for the Startec plant in the figure below is not substantiated and lower than the actual. At the time of writing, the issue remained under investigation.



Source File: KKFigures.FOSFindings.1CS019.018.rev00.xlsx

Figure 8-6: Arctic Foundation and Startec Plant Power Consumption

8.1.5 Freeze Plant COP

The following sections provide a summary of the calculated COP to the end of July 2011 for each freeze plant. For both plants, the ground heat extraction was calculated as the sum of heat extracted at each pipe.

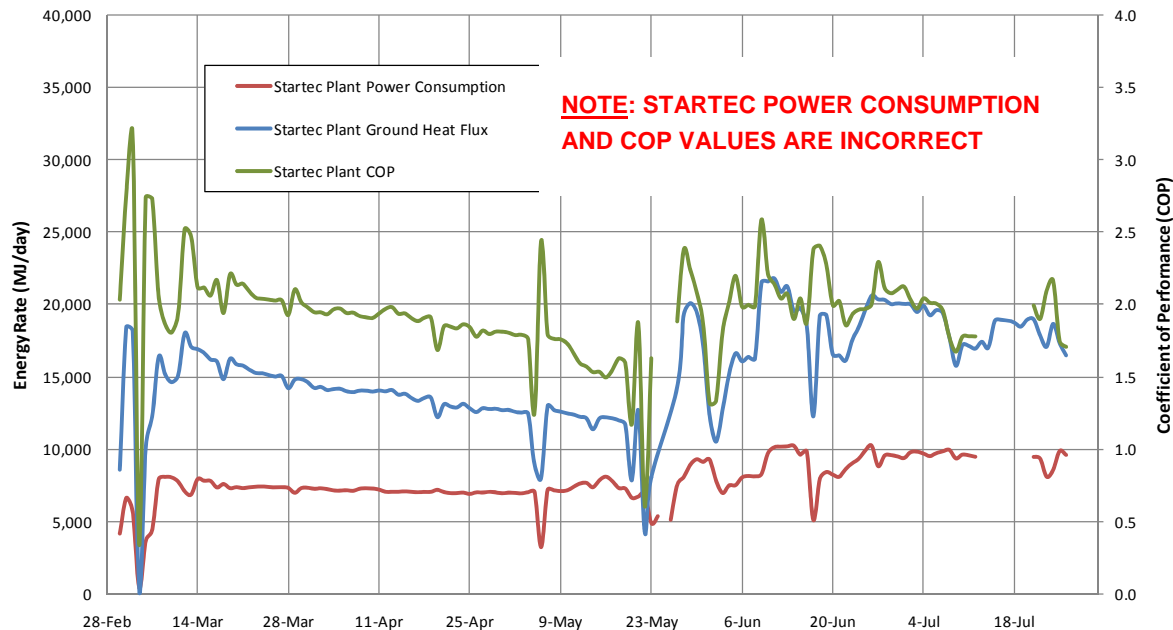
Startec Plant

NOTE: The power meter discrepancy noted in the Power Requirement Section directly impacts the COP calculations. The highlighted COP values below are not substantiated and will be updated once the power issue is resolved.

Figure 8-7 provides the calculated COP for the Startec plant since the start of the ground freezing. Following commissioning from March 2 to 7, 2011, the Startec system was operating with Groups A, C, M on the East Loop and all freeze pipes on the Underground Loop activated (the West Loop was shut off after commissioning). There were a total of 24 freeze pipes in operation with a total pipe length of 1,250 m. The supply and return distribution pipes are insulated except for the connections between surface and underground. The COP steadily decreased following activation until mid-May when Groups E and H were activated.

The eight freeze pipes of Groups E and H were activated in stages between May 29 and June 9, 2011. The activation increased the total length of the freeze pipes by 60% to 2,005 m and resulted in an increase in the COP. Since then, the COP has similarly decreased in value to the end of July 2011.

Power outages and gaps in the power consumption data are noted on Figure 8-6 and result in abrupt changes in the COP data.



Source File: KKFigures.FOSFindings.1CS019.018.rev00.xlsx

Figure 8-7: Startec Plant Coefficient of Performance Versus Time

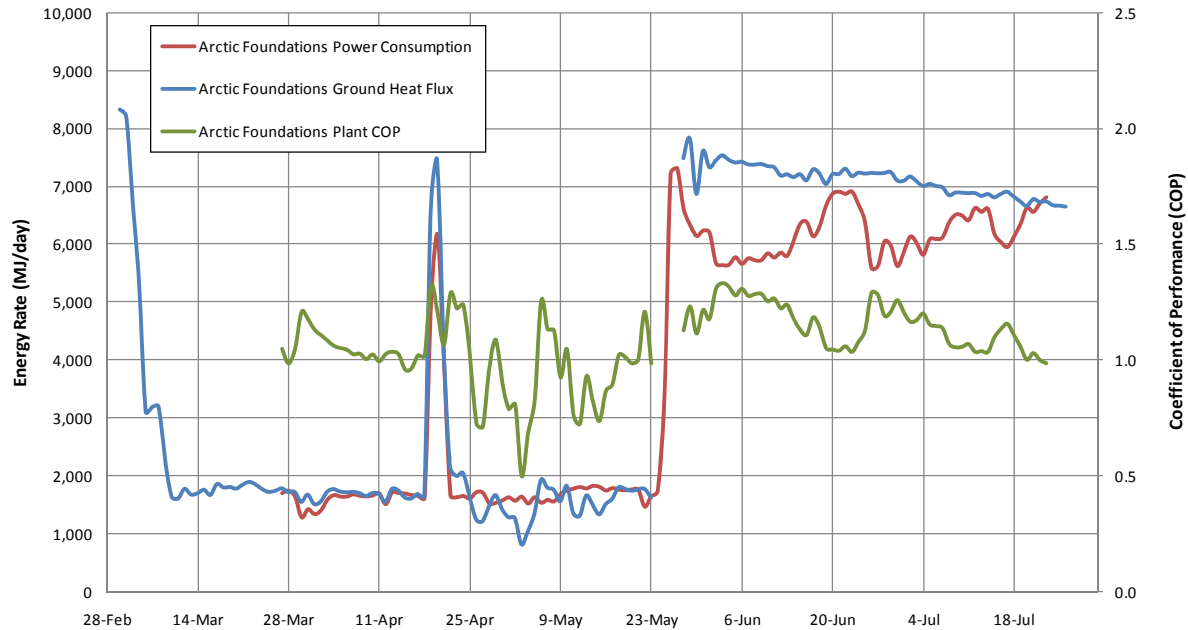
Arctic Foundations Plant

Figure 8-8 provides the calculated Coefficient of Performance (COP) for the AFCI plant since the start of ground freezing. No COP data is available prior to March 27, as the power consumption was not being tracked by the data historian. Therefore, the current COP calculations for the AFCI plant do not include heat extracted passively during the periods of cold weather at the start of the ground freezing. By including the passive contribution, the calculated COPs for the hybrid units could significantly increase.

During commissioning, Groups B, F, and G were operated actively from March 2 to 9, 2011. Refrigerant Coils A and B were both operated for each hybrid thermosyphon during commissioning. From March 9 to April 19, only Group B was operated in active mode and only with Coil A in operation. Collection of power data from the AFCI plant has been available since March 27. During this initial period COP ranged from 1.2 to 1.0.

Between April 20 and May 25, 2011, the COP was highly variable ranging from 0.5 to 1.5. During this period, Group B was operated actively with Coils A and B both turned on. The large spike in power consumption and heat extraction on April 19 and 20 was due to Groups F and G operating actively as AFCI was on site to check system performance. The oscillations were due to a large variability in the refrigerant flow through the coils. On May 26 to 28, adjustments were made by AFCI to the thermal expansion valves that resulted in a steadier flow and a corresponding steadier and higher heat extraction rate.

Groups F and G were activated on May 25, 2011. The COP increased at this time to 1.3 and has since generally decreased, ranging typically from 1.0 to 1.1 in late July.



Source File: KKFigures.FOSFindings.1CS019.018.rev00.xlsx

Figure 8-8: Arctic Foundations Plant Coefficient of Performance Versus Time

8.1.6 Active Heat Transfer Coefficients

Methodology

The theoretical heat transfer coefficient between the cooling fluid and the pipe's internal surface can be estimated by:

$$h = \frac{Nu K}{D_o} \quad (\text{Eq. 6})$$

where Nu is the Nusselt number, K is the fluid thermal conductivity, and D_o is the effective hydraulic diameter of the pipe (Newman and Lam, 2000). The hydraulic diameter is equal to the inside diameter of the steel pipe minus the outside diameter of the HDPE (high density polyethylene) Dynalene supply pipe that runs down the inside of each freeze pipe.

Table 8-5 provides the theoretical heat transfer coefficients for J55 (four inch diameter) pipes and three inch diameter pipes. The Nusselt number (4.1) and the Dynalene thermal conductivity ($39.2 \text{ kJ m}^{-1} \text{ day}^{-1} \text{ }^{\circ}\text{C}^{-1}$ at a temperature of -35°C) are the same for both pipe sizes. As the hydraulic diameter for the three inch pipes are less than the J55 pipes (0.030 versus 0.054 m), the theoretical heat transfer coefficient is expected to be larger.

The paragraphs below the table describe how the heat transfer coefficient is estimated from the pipe instrumentation.

Table 8-5: Theoretical Heat Transfer Coefficients for Three and Four Inch (J55) Pipes

	4 Inch - J55 Pipes (Groups A, D, E, H, J, K, L)	3 Inch Pipes (Groups C, M)
Steel Pipe OD (mm)	114	89
Steel Pipe ID (mm)	102	78
HDPE pipe OD (mm)	48	48
Hydraulic Diameter, D_o (mm)	54	30
Dynalene Thermal Conductivity, k ($\text{kJ m}^{-1} \text{day}^{-1} \text{ } ^\circ\text{C}^{-1}$)	39.2	39.2
Nusselt Number, N_u	4.1	4.1
Theoretical Heat Transfer Coefficient, h ($\text{kJ m}^{-2} \text{day}^{-1} \text{ } ^\circ\text{C}^{-1}$)	2,978	5,360

The convective heat transfer between the cooling fluid and the outside of the freeze pipe can be represented by the following formula:

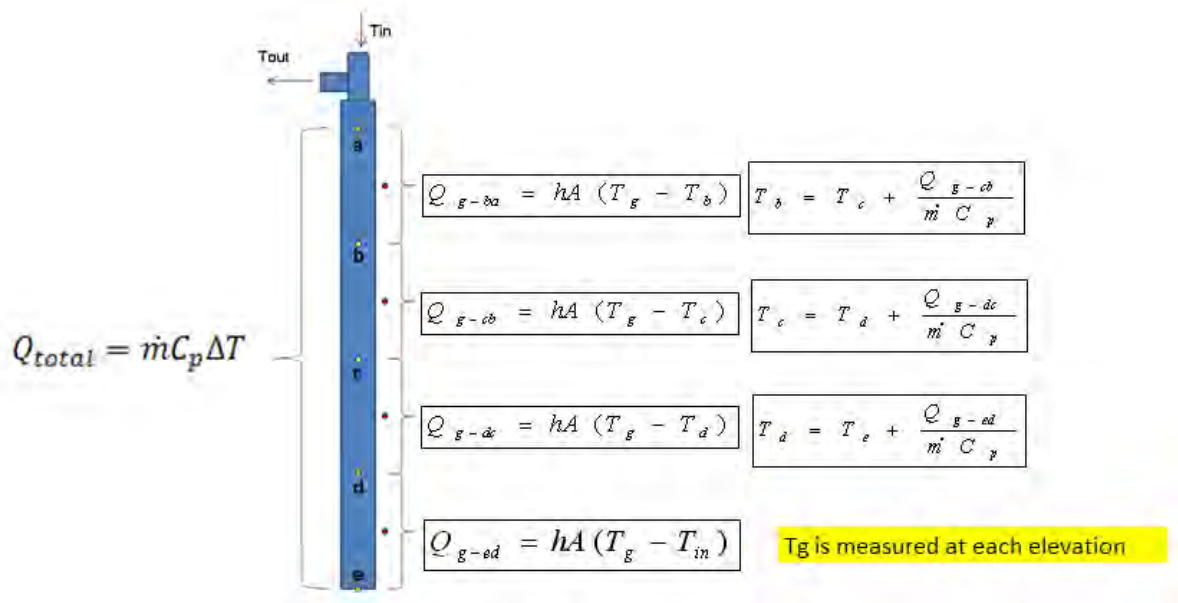
$$q_n = h (T_{gn} - T_{fn}) \quad (\text{Eq. 7})$$

where q_n is the heat flux per unit area ($\text{kJ m}^{-2} \text{day}^{-1}$), h is the convective heat transfer coefficient ($\text{kJ m}^{-2} \text{day}^{-1} \text{ } ^\circ\text{C}^{-1}$) and T_{gn} the outside pipe temperature at the depth n , and T_{fn} is the Dynalene fluid temperature at depth n .

The measurement of ground temperature at intervals along the outside of the pipe allows the heat transfer coefficient to be calculated. The 11 temperature sensors on each thermistor string provide 11 points where the pipe temperature is known, and provides a series of 11 equations with 13 unknowns: q , h , and T_f at 11 points. If the pipe temperature measurements are applied over a representative area and summed, the total flux must equal the total flux measured based on the measured flow rate and difference in brine temperature:

$$Q_{total} = \sum_{n=1}^{11} q_n A_n \quad (\text{Eq. 8})$$

Assuming that the lowest thermistor sensor is at the bottom of the hole and that the Dynalene temperature at the bottom of the pipe is equal to the supply temperature measured at the top of the hole, the series of equations may be solved iteratively for h . The concept is illustrated in the Figure 8-9.



Source File: DataManagementPlan.Figure.1CS019.018.rev00.xlsx

Figure 8-9: Heat Transfer Coefficient Calculations

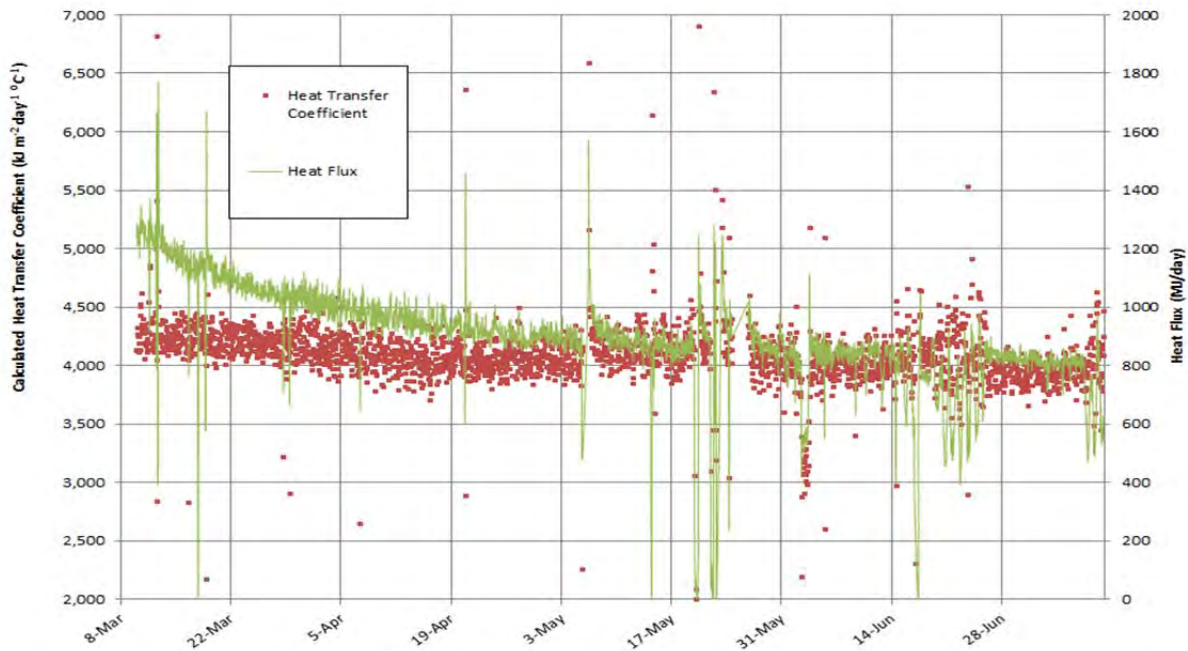
Heat Transfer Coefficient Results

Table 8-6 presents the typical heat transfer coefficient calculated for each freeze pipe at the end of June 2011. The heat transfer coefficient values reported in Table 8-6 are generally greater than the theoretical values in Table 8-6. Figure 8-10 provides an example of the calculated heat transfer coefficient for pipe P38 since the start of freezing. The calculated values show a small decreasing trend that is also observed for all of the other freeze pipes.

This trend may be due to changes in the properties of the Dynalene. As the Dynalene temperature decreases, so does its thermal conductivity. Therefore, as the Dynalene temperature decreases in the pipe, the heat transfer coefficient also decreases. As ground freezing continues, it is expected that the heat transfer coefficients will be further reduced towards their theoretical values at -35 °C.

Table 8-6: Heat Transfer Coefficient Summary

Hole	Group	Pipe Diameter (m)	Avg. Calculated Value – Sept 2011 (kJ m ⁻¹ day ⁻¹ °C ⁻¹)
P01	A	0.114	4,075
P38	A	0.114	3,750
P08	C	0.076	6,700
P14	E	0.114	2,340
P15	E	0.114	3,760



Source File: P38HeatTransferCoef.Figure.pm.1CS019.018.rev00.xlsm

Figure 8-10: P38 - Heat Transfer Coefficient versus Time

The heat transfer coefficient in an annular flow path is sensitive to the hydraulic diameter. The hydraulic diameter calculation assumes that the HDPE pipe runs down the center of the freeze pipe. However, the HDPE pipe is likely resting against the wall of the steel pipe in some areas due to bends in the pipe. The heat transfer coefficient may therefore vary, and contribute to an irregular temperature trend along the pipe, depending on the position of the thermistors on the outside of the steel pipe with respect to the location of the HDPE pipe.

The difference in calculated heat values among the Group E freeze pipes shows this potential variability of the heat transfer coefficient. Table 8-7 summarizes the average supply and return temperatures for pipes P14 and 15 for the month of July. The supply temperature averaged 0.25 °C warmer in P14 compared to P15, while the return temperature averaged 0.5 °C cooler in P14 compared to P15. This resulted in the change in temperature for P15 being approximately 40% higher than P14. The resulting heat transfer coefficient was 60% higher.

Measurement error of the thermistors, RTDs, and/or flow meters is not likely to be the cause of the differences between P14 and P15. However, for P15, the Dynalene temperature supply RTD sensor (TI_P15_012) malfunctioned, and as a result, the supply temperature for P12 was used in the above heat transfer coefficient calculations. The P12 supply temperature was chosen as the values are most representative of the Group E average supply temperature.

Table 8-7: Group E Average Dynalene Temperatures – Sept 2011

	P14	P15
Dynalene Supply Temperature (°C)	-34.12	-34.37
Dynalene Return Temperature (°C)	-32.31	-31.83
Change in Temperature	1.81	2.54

8.2 Hybrid Thermosyphon Pipe Diameter

Groups B, F and G each contain four hybrid thermosyphons, but with each Group having a different pipe diameter. Group B pipes are 3 inches in diameter, Group F pipes are 4 inches in diameter, and Group G pipes are 2.5 inches diameter.

Based on the predicted passive heat flux equation presented in Section 5.3.2, the pipe diameter is not expected to affect performance. A range of pipe diameters was included in the study to examine the influence of the pipe diameter on performance. Specifically they were included to confirm that the CO₂ within the pipe circulates along the entire length of the pipe and that pipe temperatures are similar amongst all of the groups.

This section presents a comparison of pipe temperatures between Groups F and G. Figure 8-11 and Figure 8-12 compare pipe temperatures from Groups F and G during the passive and active periods. Group B was not included in the comparison as explained later in this section.

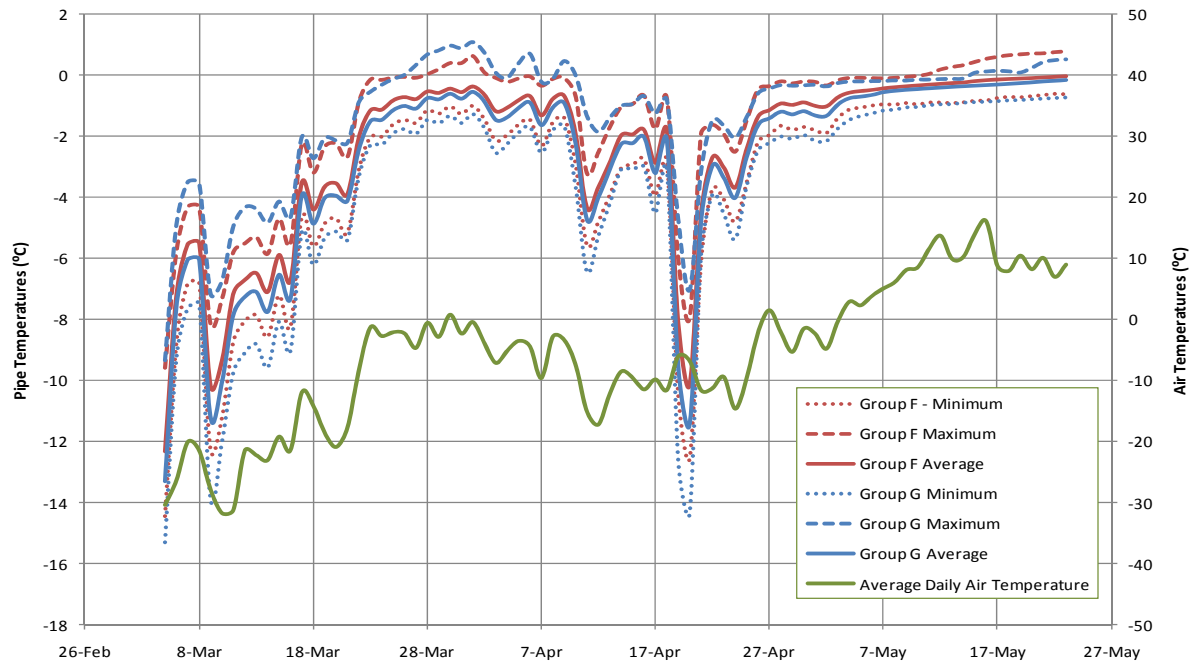
These groups provide a good comparison as they are the extremes of the pipe diameters used in the study and have been operated under the same conditions throughout the study. Both were operated passively from the start of the study until May 25, 2011, when they began to be operated actively.

Each figure plots the average maximum and minimum pipe temperatures recorded by all pipe temperature sensors along each pipe. Each group contains three pipes with thermistor strings with 11 temperature sensors each. The top sensors for each pipe were excluded from the calculations as they are located close to the ground surface and are influenced by the surface temperature.

The figures show that the difference in performance between Groups F and G is negligible. The average pipe temperature for Group G was 0.1 °C cooler than Group F during the last few weeks of the passive period and 0.8 °C cooler during the active period in July 2011. (July temperatures only were compared as pipe P23 of Group G operated with only one coil active in June).

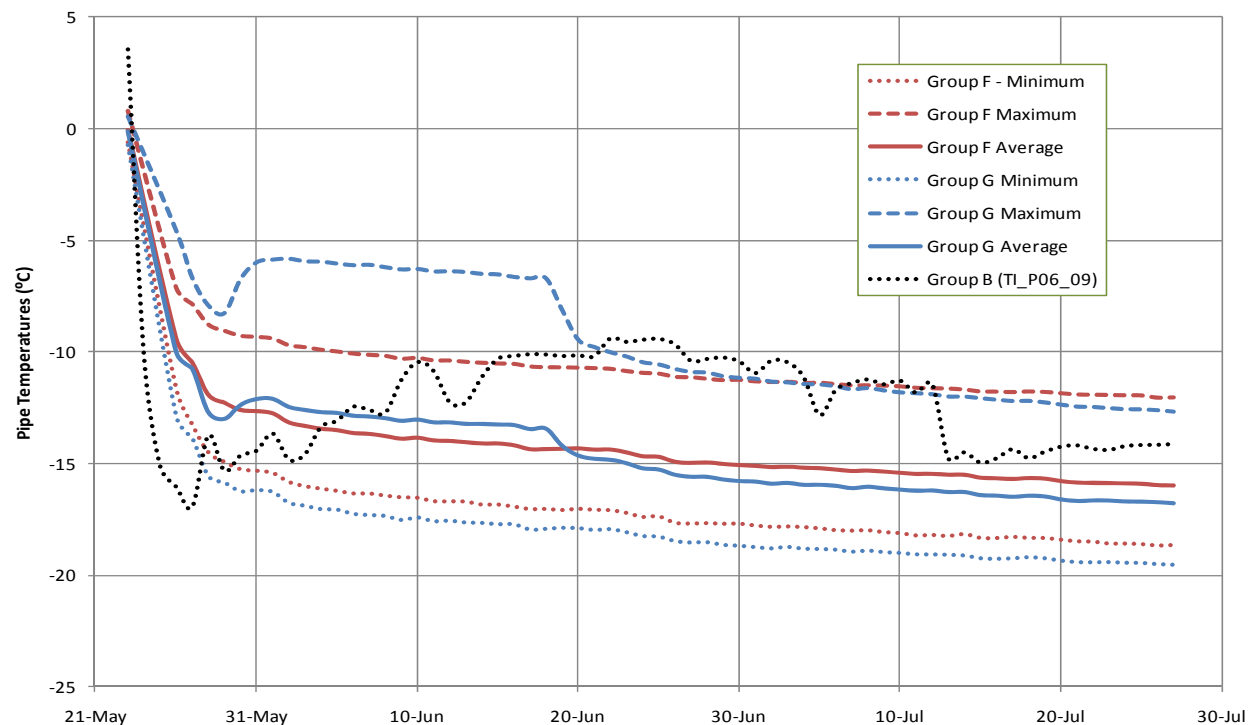
Group B was not included in the comparison as it had been operating actively since the start of the study and was operating for a period with only one coil active. To illustrate why Group B was not used in the comparison of pipe sizes, a typical Group B pipe temperature sensor (TI_P06_009) is included with active operation of Groups F and G in Figure 8-12. Sensor (TI_P06_009) was chosen to be representative of Group B, as the temperatures are the closest to the average pipe temperature for the group.

For comparative illustration purposes, the first day of active operation of Group B (February 28, 2011) was adjusted to coincide with the first day of active operation for Groups F and G (May 25, 2011). Group B initially cooled more quickly than Groups F and G due to the cooler weather during March compared to late May. Group B pipe temperature then increased due to warmer weather, only one refrigerant coil being in operation, and inconsistent refrigerant flow.



Source File: KKFigures.FOSFindings.1CS019.018.rev00.xlsx

Figure 8-11: Hybrid Thermosyphon Performance Comparison of Groups F and G During Passive Operation



Source File: KKFigures.FOSFindings.1CS019.018.rev00.xlsx

Figure 8-12: Hybrid Thermosyphon Performance Comparison of Groups F and G During Active Operation

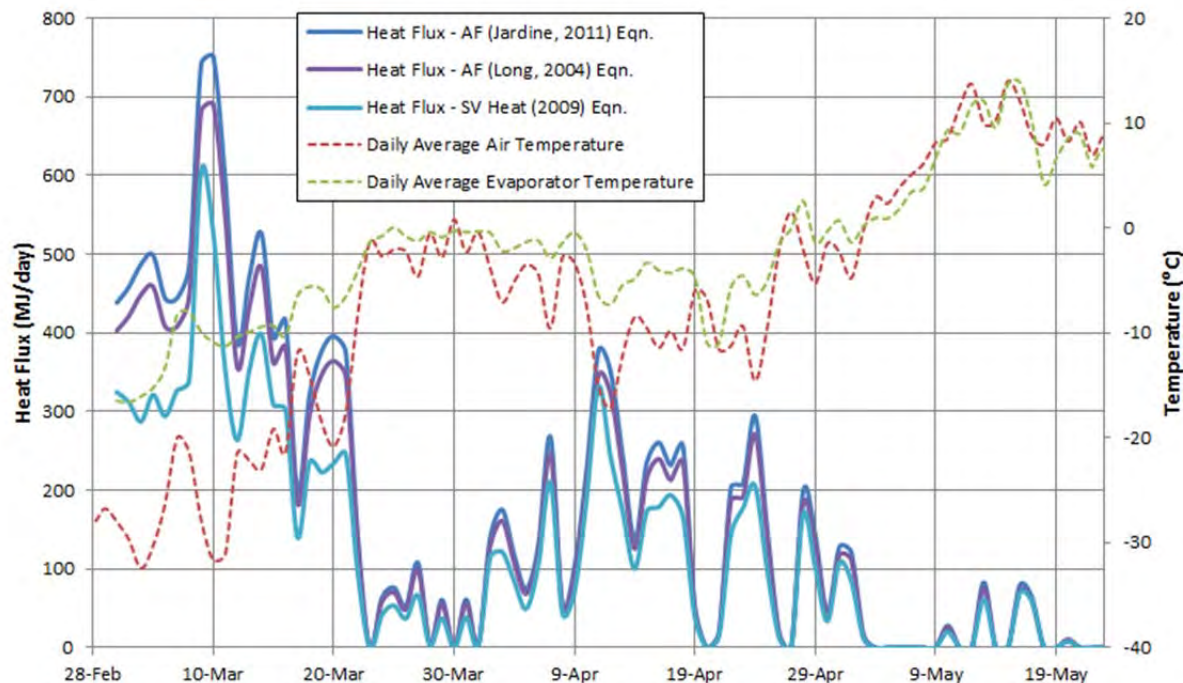
8.3 Passive Thermosyphon Heat Flux

8.3.1 Comparison of Predicted Flux Formulas

Section 5.3.2 detailed the calculation of the predicted passive thermosyphon heat flux and presented three sets of heat transfer coefficient formulas. This section provides a comparison of the predicted flux using each formula.

For average daily air temperature colder than -10 °C (when the thermosyphons would be operating), the average wind speed measured as part of the FOS has been 1.7 m/s. SRK (2006) reports an average wind speed of 2.3 m/s at the experimental thermosyphon for this temperature. At this wind speed range, the resulting heat flux using the 2011 AFCl equation is approximately 20% higher than the predicted flux used during the conceptual design.

Figure 8-13 provides a comparison of the estimated heat flux for the Group F hybrid thermosyphons operating in passive mode. The daily averaged parameters of evaporator temperatures, air temperatures and wind speeds were used to generate a set of the daily average heat extraction rate. Differences among the heat flux formulas are not as pronounced under dynamic conditions. However, where a large temperature gradient exists, the differences in predicted heat flux can be significant.



Source File: PMFigures.FOSFindings.1CS019.018.rev00.xlsx

Figure 8-13: Passive Thermosyphon Heat Flux – Group F

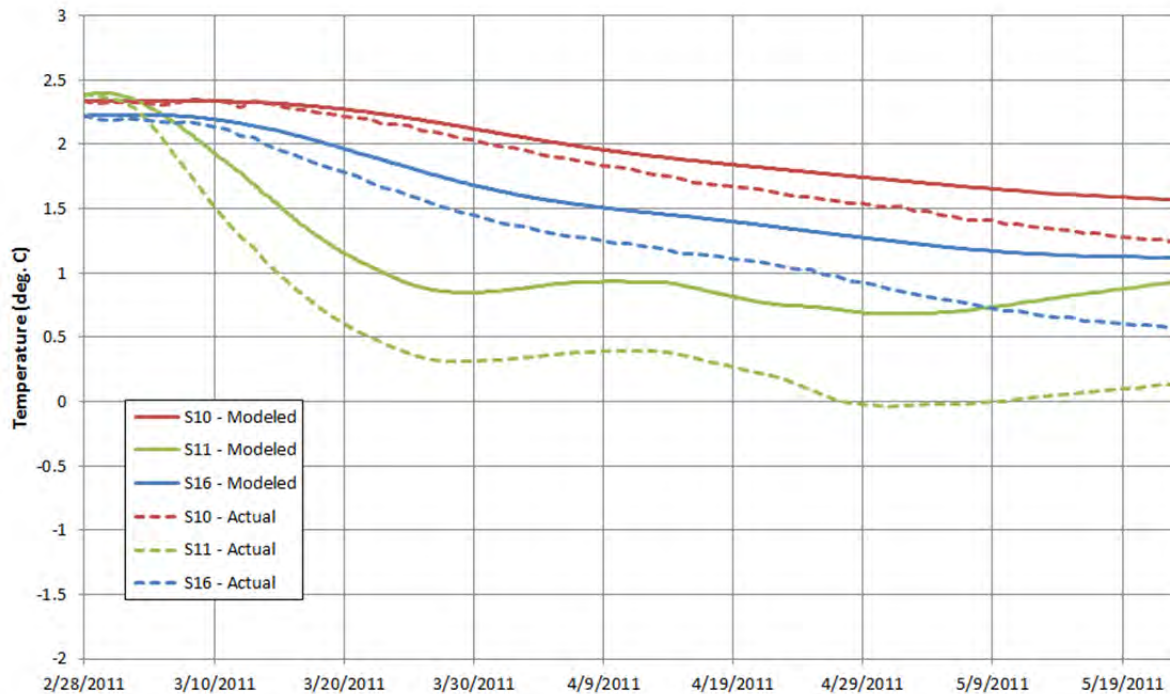
8.3.2 Comparison of Predicted Flux to 2D Model, Groups F and G

A simulation was completed using the daily averaged heat flux for each hybrid thermosyphon in Groups F and G over the period of passive operation. The general model set up is described in Section 9.1.2. The major differences for this simulation are that the model was run only during the period of the passive thermosyphon operation and that all other freeze pipes were omitted.

The heat flux boundary condition for each thermosyphon was estimated using the AFCI 2011 parameters (Set 3 in Table 5-1). As mentioned in the previous section, the daily averaged parameters of pipe temperatures, air temperatures and wind speeds were used to generate a set of the daily average heat extraction rate. The thermosyphons were operated passively from March 5 to May 24, 2011. Groups F and G were operated actively from February 28 to March 5 and April 19 to May 21, which makes the predicted values during these periods incorrect.

The bedrock was assigned a typical thermal conductivity of $400 \text{ kJ day}^{-1} \text{ m}^{-1} \text{ }^{\circ}\text{C}^{-1}$ and a thermal diffusivity of $0.16 \text{ m}^2/\text{day}$, which was found to have the best fit for instrumentation holes S10, S11 and S16.

Figure 8-14 provides a comparison of the temperature responses at these three instrumentation holes. The figure shows that the AFCI (2011) equation underestimates the heat flux from the thermosyphons as the modeled rates of cooling are less than observed. No simulations were completed using the other predictive flux parameters as they would also result in underestimated flux.



Source File: Figure.ThermosyphonFluxTempComp.1CS019.018.rev00.xlsx

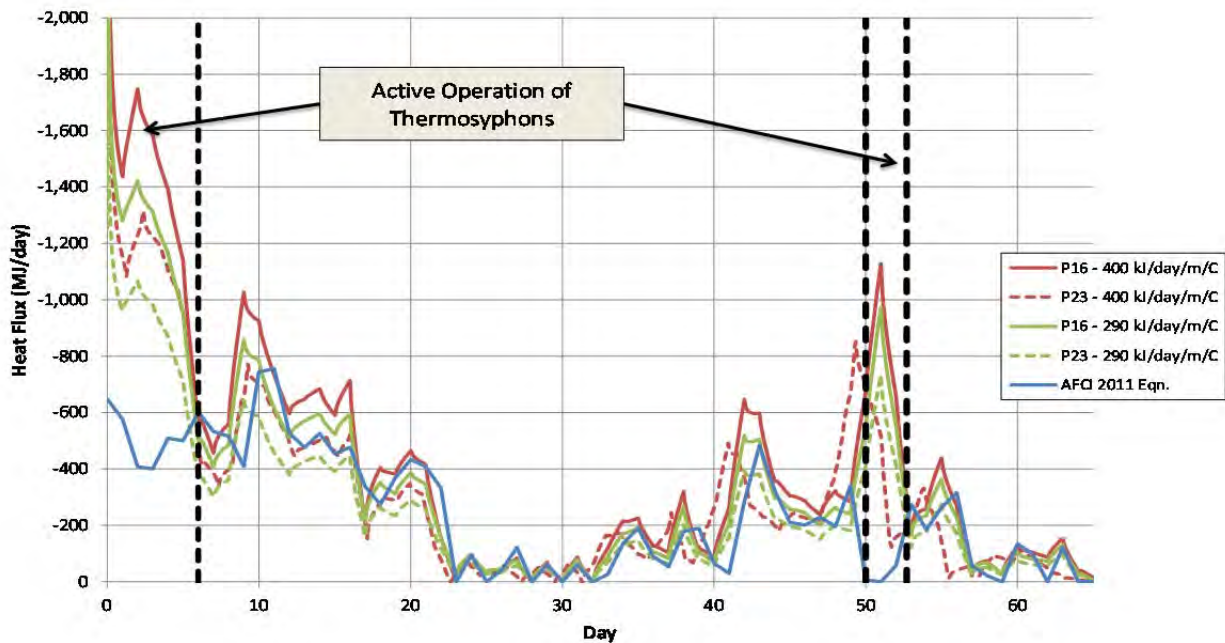
Figure 8-14: Comparison of Temperature Responses for Modeled and Theoretical Passive Thermosyphon Heat Flux

Simulations were also completed that used measured Group F and G pipe temperatures to estimate the heat flux from each thermosyphon. A sensitivity analysis was completed to estimate the range of flux. The analysis considered the following range of bedrock properties:

- The mineralogy results presented in Section 8.1.1 estimated a typical thermal conductivity of $400 \text{ kJ day}^{-1} \text{ m}^{-1} \text{ }^{\circ}\text{C}^{-1}$, with a possible low estimate of $290 \text{ kJ day}^{-1} \text{ m}^{-1} \text{ }^{\circ}\text{C}^{-1}$;
- The thermal diffusivity modeling presented in Section 8.1.2, estimated diffusivities ranging from 0.13 to $0.16 \text{ m}^2/\text{day}$ in the Group F and G area; and,
- The above properties result in heat capacities ranging from of 2.23 to $3.07 \text{ MJ m}^{-1} \text{ }^{\circ}\text{C}^{-1}$.

The sensitivity analysis found that the predicted fluxes were the most sensitive to the thermal conductivity, with little change resulting from variance in the heat capacity.

Figure 8-15 compares the range of modeled heat flux using thermal conductivities of 400 and 290 $\text{kJ day}^{-1} \text{ m}^{-1} \text{ }^{\circ}\text{C}^{-1}$ to the AFCI (2011) predictive flux equation provided by John Jardine. The periods of active operation of the thermosyphons are also noted. During cold weather periods and for the typical thermal conductivity of $400 \text{ kJ day}^{-1} \text{ m}^{-1} \text{ }^{\circ}\text{C}^{-1}$, the theoretical heat flux falls within the range of the modeled extraction rates for Groups F and G, but similar to the model presented in Figure 8-14, generally underestimates the heat flux..



Source File: ThermosyphonFluxCoefficientFitting.1CS019.018.rev00.xlsx

Figure 8-15: Comparison of Modeled to Theoretical Passive Thermosyphon Heat Flux

Table 8-8 compares the cumulative heat flux between March 10 to April 17. These dates were selected to exclude any influence from active operation. The results shown assume a bedrock thermal conductivity of $400 \text{ kJ day}^{-1} \text{ m}^{-1} \text{ }^{\circ}\text{C}^{-1}$ and a diffusivity of $0.16 \text{ m}^2/\text{day}$. The comparison shows that on average, the modeled heat flux was 10% greater than predicted by the AFCI (2011) equation.

Table 8-8: Comparison of Predicted Thermosyphon Heat Flux

	Minimum Flux (MJ)	Average Flux (MJ)	Maximum Flux (MJ)
AFCI 2011 Equation Flux	8,769	9,404	9,896
Modeled Flux	8,926	10,317	11,387
Difference	1.8%	9.7%	15.1%

Source File: ThermosyphonFluxCoefficientFitting.1CS019.018.rev00.xlsx

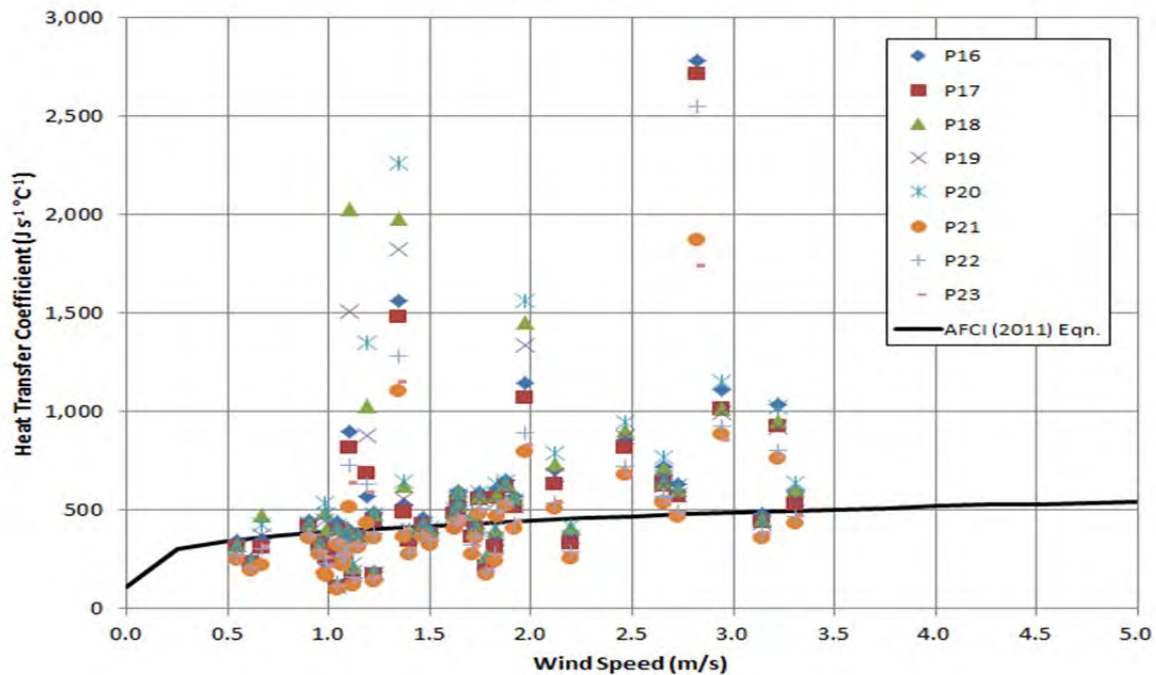
8.3.3 Thermosyphon Heat Transfer Coefficient

An investigation was completed to determine if alternative curve fitting parameters would provide a better match to the model results. Figure 8-16 plots the modeled heat transfer coefficient for each pipe as a function of wind speed. The plotted heat transfer coefficient was calculated as in Equation 5, as the modeled heat flux divided by the difference in measured pipe and air temperatures. Also plotted is the AFCI (2011) heat transfer coefficient equation.

The plot shows that there is considerable scatter of the modeled heat transfer coefficients. Most outliers with high coefficients occur when the difference between the average daily air and pipe temperatures is small. Values of h when the temperature difference is less than $0.3 \text{ }^{\circ}\text{C}$ were omitted from the plot.

At wind speeds, higher than 2 m/s , the AFCI (2011) equation generally under predicts h , however, at this time, the sample size is small and the results may change with additional data. At the average wind speed range (1.7 and 2.3 m/s), the equation appears to provide a slightly conservative fit.

Given the scatter of the data, the AFCI (2011) equation appears to be appropriate for use in future design work. The coefficients provide a slightly improved performance compared to the Long (2004) equation used for the SRK (2006) conceptual design.



Source File: ThermosyphonFluxCoefficientFitting.1CS019.018.rev00.xlsx

Figure 8-16: Passive Thermosyphon Heat Transfer Coefficients

8.4 Active Freeze Pipe Diameter and Completion Detail Comparison

Most of the active freeze pipe groups consist of four inch diameter J55 steel pipes. The exceptions are Group C, with three inch diameter pipes grouted into raw holes and Group M with three inch pipes grouted inside four inch J55 pipes. Groups A, C, and M were all activated at the same time to provide a direct comparison of active freezing performance using the different pipe sizes and grouting details. Activation of Groups E and H (four inch diameter J55 pipe) started on May 24, 2011 and followed a staggered ramping up to full flow in all pipes over a two week period.

Of the active freeze pipes, Groups A, C, and E have thermistor strings installed along the outside:

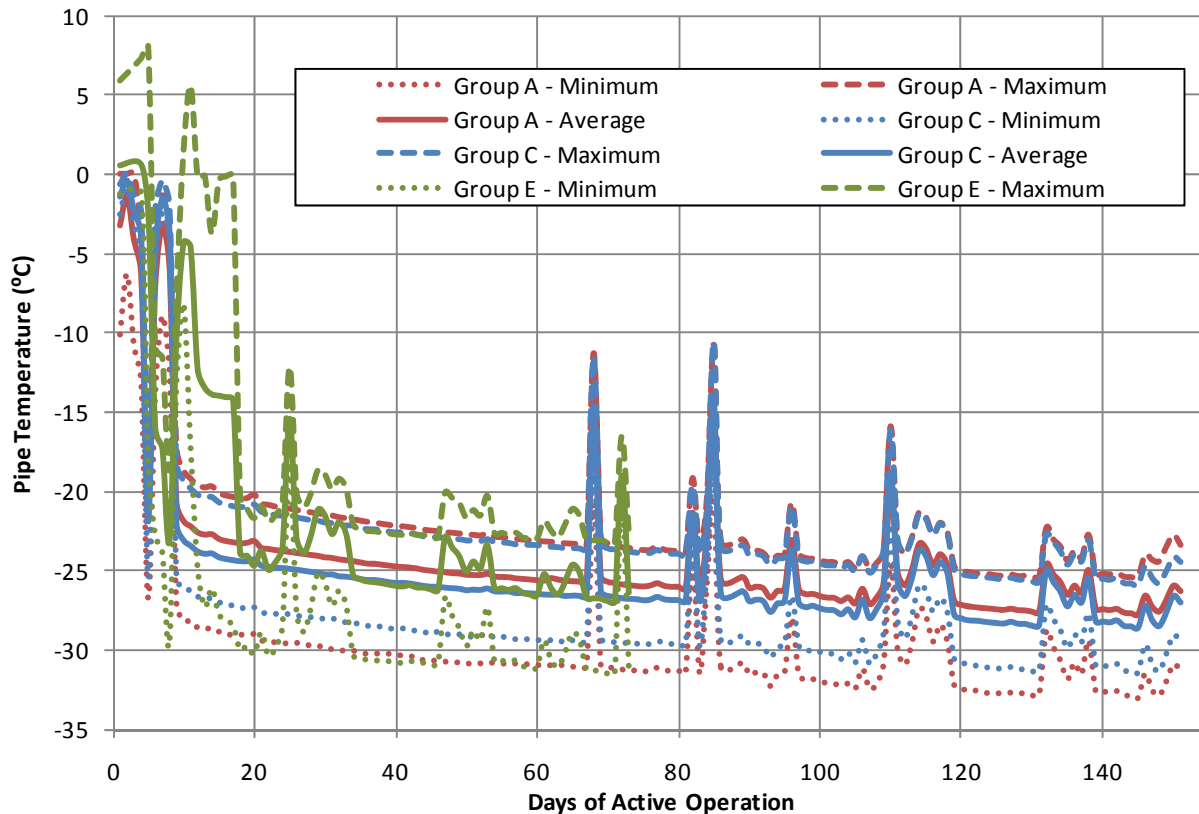
- Group A: P38 and P01 (the 1st and 2nd pipes, respectively, in the series of two)
- Group C: P08
- Group E: P12, P14, and P15

Figure 8-17 plots the minimum, average and maximum of the temperature sensor responses for each freeze group following the activation. Day one for Groups A and C was February 28, 2011; Day one for Group E was May 24. The top temperature sensors for P01 (Group A) and P14 (Group E) were excluded from the calculations due to their close proximity to the ground surface.

Spikes in the temperature responses generally occurred during plant maintenance shutdowns or power outages and during periods when the ambient air temperature exceeded +20 °C. The warm air temperatures have been resulting in a corresponding increase in the supplied Dynalene temperature from the Startec freeze plant.

Excluding the temperature spikes, the pipe temperatures measured in Group C and Group E are nearly identical. The data suggests that the pipe diameter has little influence of the freeze results.

Pipe temperatures for Group A are more variable compared to Group C with an average pipe temperature typically 0.6 °C warmer. The differences in temperature are more likely to be due to the piping arrangement: serial vs. parallel connections. The flow rate of Group A at 2.7 m³/hr is lower than Groups C and E at 3.4 m³/hr. This is due to the series arrangement of pipes in Group A that effectively doubles the length of pipe and friction losses along the Dynalene flow path. The longer contact time of the cooling fluid in the Group A pipes results in a higher average temperature inside the pipe and a lower temperature differential between the cooling fluid and outside the pipe.

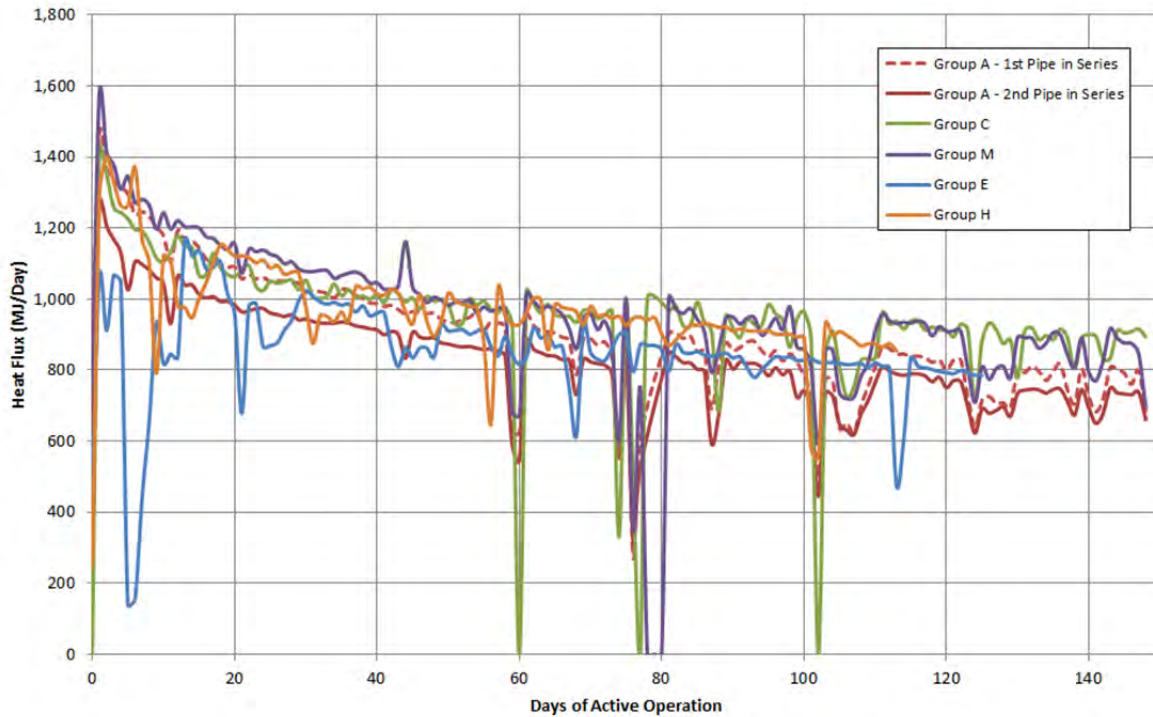


Source File: PMFigures.FOSFindings.1CS019.018.rev00.xlsx

Figure 8-17: Comparison of Active Freeze Pipe Temperatures

Figure 8-18 plots the daily average heat flux (MJ/day) for each active freeze group. For Group A, the daily averaged fluxes were calculated between each pipe with the same positioning in the series, i.e., first pipes in series and second pipes in series. The differences between Groups A and C are discussed above, and can be attributed to the lower coolant flow rate in Group A.

Differences in the flux rates between Groups E and H during the initial stages of activation were due to their staggered activation schedule. Groups E and H were activated between May 27 and June 9, 2011 to prevent excessive loading on the freeze plant. Figure 8-18 plots day one as June 3 for Group E and June 7 for Group H. Flux rates for Group H (4 inch diameter) are similar to those of Groups C and M (3 inch diameter) when the Startec freeze plant is operating optimally.



Source File: PMFigures.FOSFindings.1CS019.018.rev00.xlsx

Figure 8-18: Comparison of Active Freeze Pipe Heat Flux

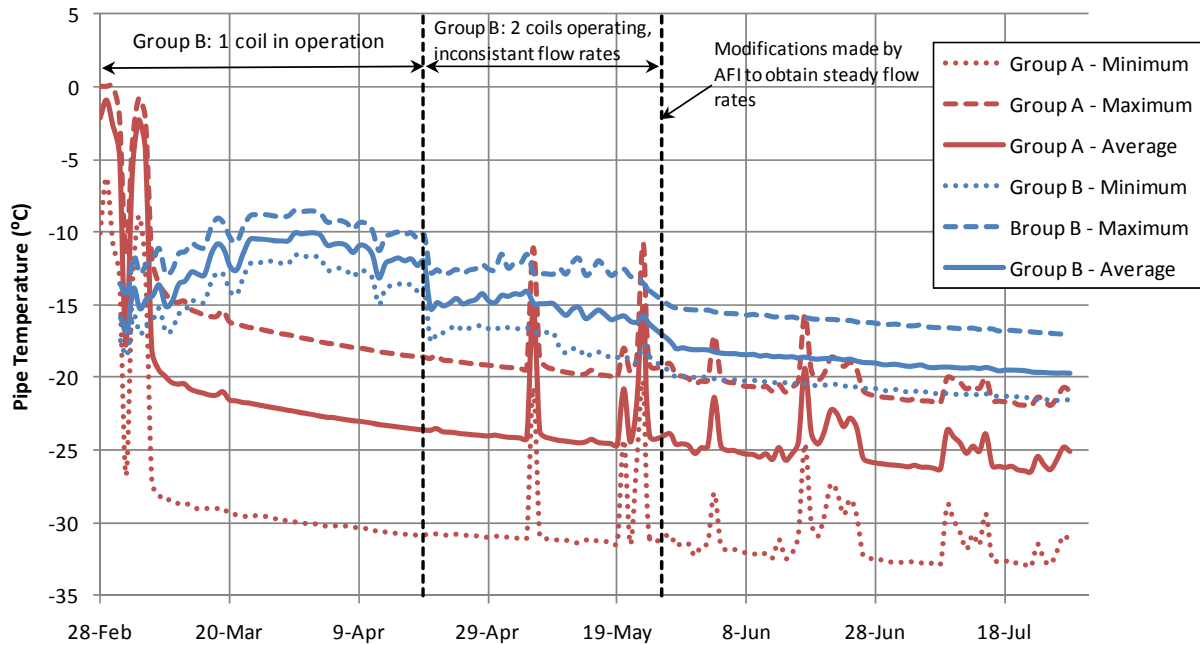
8.5 Comparison of Active Freezing and Hybrid Thermosyphon Performance

At the end of August 2011, it was too early to make a complete evaluation between the freeze technologies and the variations among each. Hybrid thermosyphon performance was not captured during the cold winter months when the hybrid thermosyphons receive the added benefit of passive cooling. Group B, which operated actively since the start of the FOS and could have provided the performance data, was not operating optimally during the initial period when weather was cold.

Figure 8-19 provides graphs plotting the minimum, average and maximum of the temperature sensor responses for Groups A and B. Group B performance to the end of July can be divided into three distinct stages:

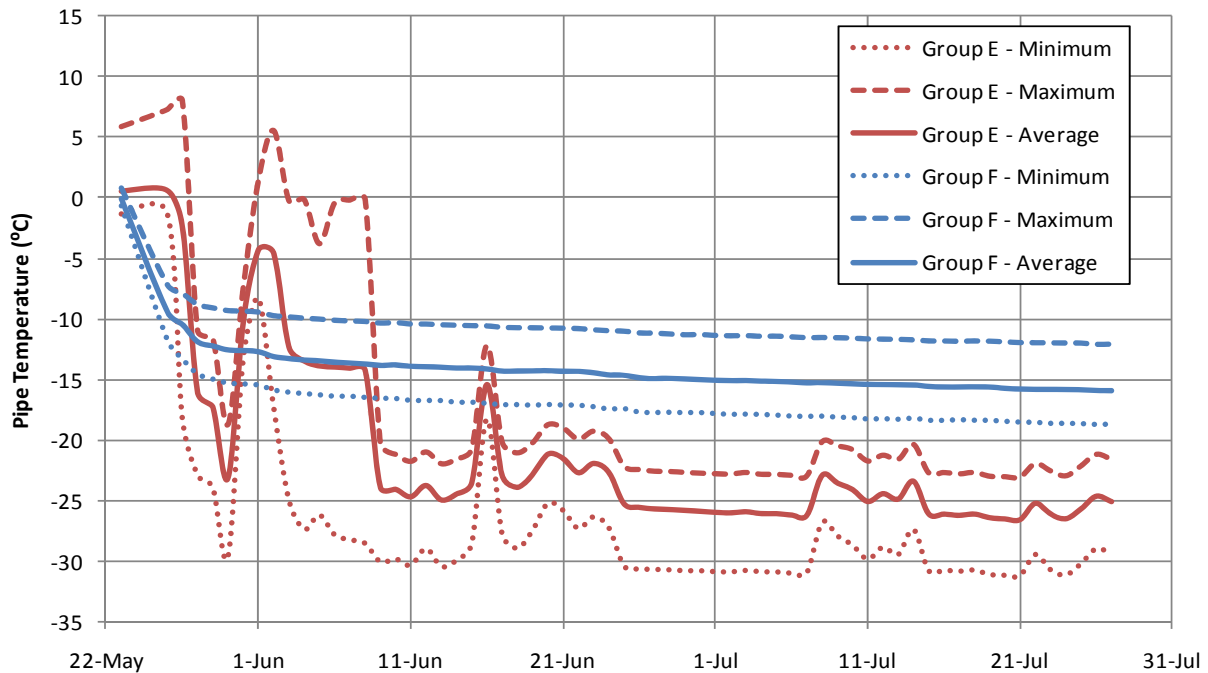
- March 9 to April 19: Following commissioning, Group B was operated using only one of two refrigerant loops, Rack A that supplies Coil A. As the weather warmed during this period and rates of passive heat removal reduced, the pipe temperatures increased.
- April 19 to May 26: On April 19, the second refrigerant loop, Rack B supplying Coil B, was activated. This resulted in up to twice the refrigerant being circulated through each hybrid thermosyphon, an increase in the overall rate of heat removal, and an immediate decrease in pipe temperatures. During this period, refrigerant flow rates were highly variable, fluctuating between 20 and 100 kg/hr though each coil. This variability was due to a faulty parameter in the flow transmitter at the AFCI freeze plant.
- May 26 to present: Modifications made by AFCI that resulted in steady flow rates (typically 80 kg/hr per coil) and cooler pipe temperatures.

Figure 8-20 provides the same comparison of pipe temperatures for Groups E and F. These groups were both activated in late May. Prior to this period Group F was operated passively with pipe temperatures generally at 0 °C. The active freezing of Group F occurred following the modifications by AFCI to the thermal expansion valve settings to obtain steadier flow rates.



Source File: PMFigures.FOSFindings.1CS019.018.rev00.xlsx

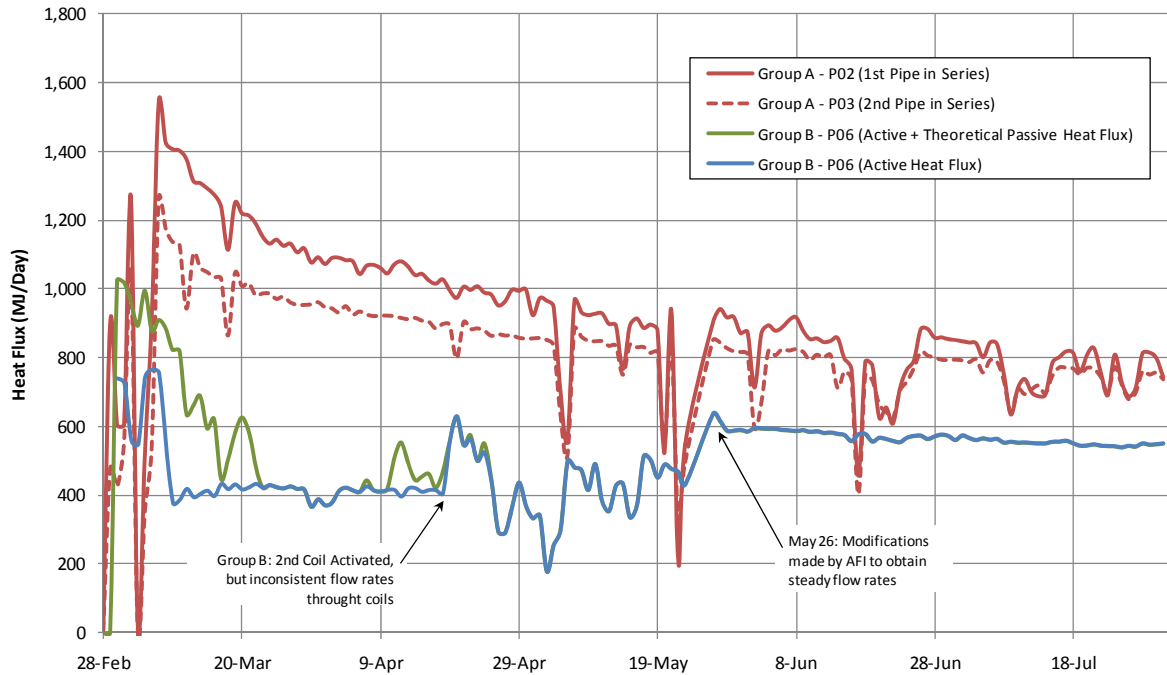
Figure 8-19: Comparison of Group A and Group B Pipe Temperatures



Source File: PMFigures.FOSFindings.1CS019.018.rev00.xlsx

Figure 8-20: Comparison of Group E and Group F Pipe Temperatures

Figure 8-21 provides a comparison of Group A and B average heat flux rate per pipe. Details of the estimated passive heat flux are provided in Section 8.3. Pipe P06 temperatures were used in the passive thermosyphon calculations as its heat flux rates and pipe temperatures best represent the average for the group. Rates were calculated based on averaged hourly wind speeds and air temperatures.



Source File: PMFigures.FOSFindings.1CS019.018.rev00.xlsx

Figure 8-21: Comparison of Active Versus Hybrid Heat Flux (Group A and Group B)

8.6 Group E Conversion

Group E consists of four pipes, P12 to P15, in the southwest area of the study. The holes consist of 4.5 inch (114 mm) J55 casing with welded joints. Following the initial active freeze, when the freeze operation reverts to maintaining the frozen condition, Group E pipes are to be converted from active freeze pipes to thermosyphons. Radiators, similar to those on the 4 inch, Group F thermosyphons, will be installed directly onto the existing pipes. The performance of the Group E thermosyphons will then be compared to the performance of other thermosyphons where the entire freeze pipe has been replaced.

8.7 Time Predictions for Initial Freeze Wall Criteria

The conceptual freeze design predicted that the initial freeze criteria for a 10 m wide, -10 °C freeze wall would be achieved in 9.5 to 11 months. The prediction was based on:

- A pipe spacing of 4 m
- Best estimates of material properties (Table 8-3)
- An initial ground temperature of 3 °C
- A 7 m offset of the freeze alignment from the arsenic chambers

- An operating brine temperature of $-30\text{ }^{\circ}\text{C}$

The findings of the FOS to date, as described in previous sections, have resulted in changes to the parameters used in the conceptual design modeling that have an effect on the time to achieve the initial criteria. These include:

- Dynalene temperature operating at a target supply temperature of $-35\text{ }^{\circ}\text{C}$.
- Bedrock thermal conductivity of $400\text{ kJ day}^{-1}\text{ m}^{-1}\text{ }^{\circ}\text{C}^{-1}$ and diffusivity of $0.15\text{ to }0.19\text{ m}^2\text{ day}^{-1}$ are higher than the conceptual modelling assumptions of $300\text{ kJ day}^{-1}\text{ m}^{-1}\text{ }^{\circ}\text{C}^{-1}$ and $0.126\text{ m}^2\text{ day}^{-1}$ respectively.
- The seven meter offset of the freeze alignment is not present around the entire perimeter of the chamber. On the north, east, and south sides of Chamber 10, the offsets are greater in order to encapsulate contaminated drifts inside of the frozen shell. The increased offset results in longer initial freeze times as the insulating effect of the arsenic chamber is reduced.

Updated model simulations were completed to the end of August 2011 using the revised parameters from the freeze study to provide revised estimates of the time to reach the initial criteria.

Simulations were completed for both active freezing and for hybrid thermosyphons. For each technology, pipes with the minimum and maximum pipe temperatures were specified to provide a range of estimates.

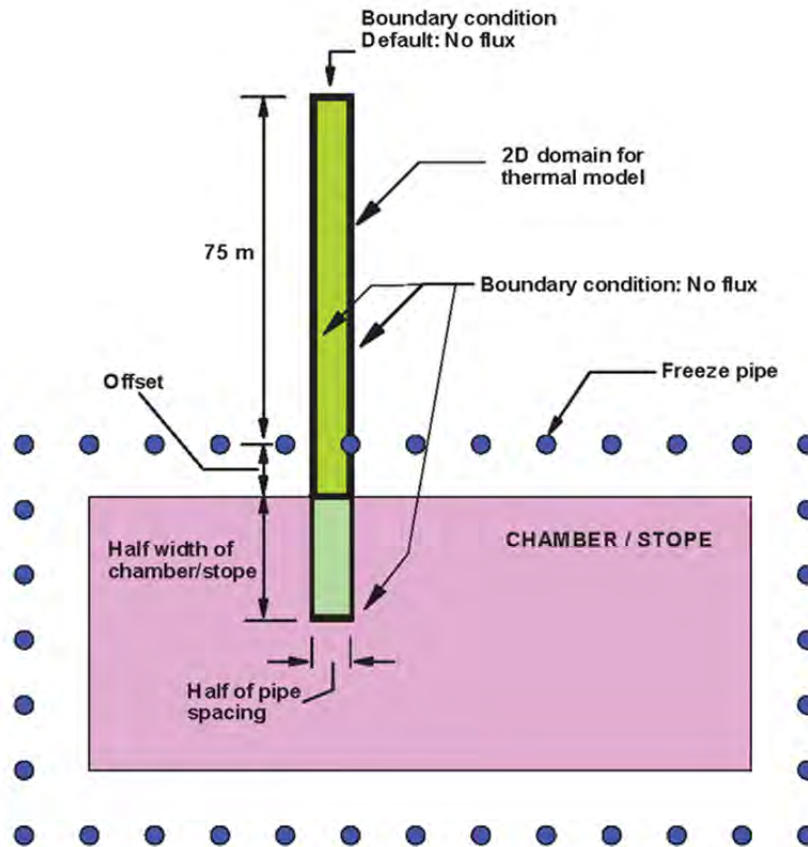
Details of the model setup are provided in Section 8.7.1. Time predictions investigating the effect of the arsenic chamber offset are presented in Section 8.7.2. Time predictions with pipe spacing ranging from four to six meters are presented in Section 8.7.3.

8.7.1 Model Setup

Model simulations were completed using SVHeat Version 6 using a 2D horizontal plane.

A schematic view of the model is provided in Figure 8-22. The model domain is the same as that used in the conceptual design for prediction of the initial freeze time. The model includes the half distance of the pipe spacing, with one boundary located midway between two adjacent freeze pipes and the other intercepting the centre of a freeze pipe. The domain extends outside of the freeze alignment to a distance of 75 m and inside of the freeze alignment to a distance halfway into the chamber or 5 m into Chamber 10. For models completed without the arsenic chamber, the domain extended 75 m on each side of the freeze alignment.

Zero flux boundary conditions were applied to all boundaries except for the freeze pipe boundary. Temperature expressions were specified along the pipe boundaries based on the daily averaged recorded pipe temperatures.



Source File: InitialCriteria2DModelSchematic.1CS019.018.tif

Figure 8-22: Schematic Plan View of the Horizontal Plane Used as the Domain for the Thermal Simulations

The pipe boundary temperature expression consisted of a curve fit applied in two stages. The first stage was applied over the first 10 days of freezing where there is a rapid decrease in pipe temperature consisting of a linear expression. The second stage was applied at all times greater than 10 days and applied an exponential decay function of the form:

$$T = A * e^{\left(\frac{-t}{f}\right)} + T_{ss} \quad (\text{Eq. 8})$$

where T is temperature (°C), A is the difference between the initial and the long-term pipe temperature (°C), t is time (days), f is a curve fitting parameter and T_{ss} is the long-term pipe temperature (°C).

The pipe boundary condition parameters are summarized in Table 8-9. For the active freeze pipes, the long-term pipe temperature was assumed to be equal to the Dynalene supply temperature of -35 °C. For the hybrid thermosyphons, the long-term temperature was assumed to be -30 °C for the CO₂.

At this early stage of the freeze study, there is a large uncertainty as to the long-term temperature for the hybrid thermosyphons. The -30 °C temperature used also does not consider the benefits of passive heat extraction which may result in cooler temperatures during the winter months. The time predictions are for active heat extraction only for the hybrid thermosyphon and are likely conservative.

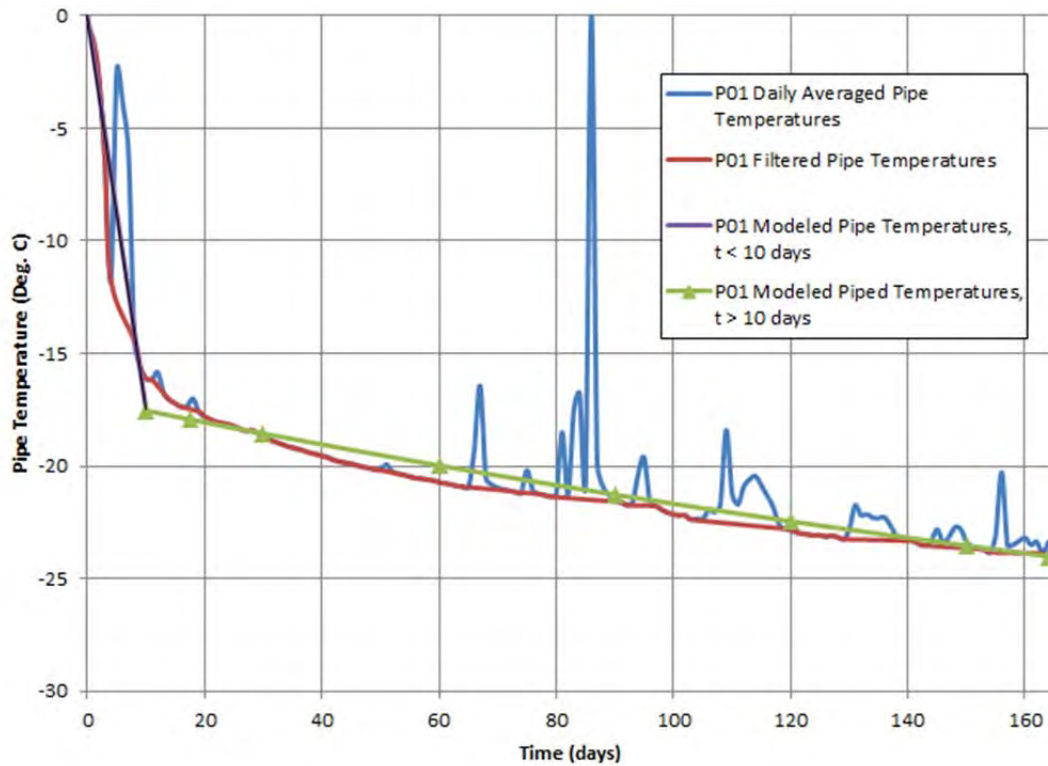
Table 8-9: Pipe Temperature Boundary Condition Parameters for Freeze Wall Time Prediction Modeling

	Pipe Boundary Condition Equation, Time < 10 days	Pipe Boundary Condition Parameters, Time >= 10 days (Eq. 8)		
		Long-term pipe temperature, T_{ss} (°C)	A, (°C)	Curve-fit Parameter, f
P01	$T = -1.75 \cdot t$	-35	18	333
P38	$T = -2.15 \cdot t$	-35	14	279
P16	$T = -0.34 \cdot t - 12$	-30	15	404
P20	$T = -0.20 \cdot t - 14$	-30	14.5	270

For the hybrid thermosyphons, pipes P20 and P16 were selected to represent the range of recorded pipe temperatures. For the active freeze pipes, P01 and P38 of Group A were selected to represent the range of recorded active pipe temperatures. P01 and P38 are connected as a pair of freeze pipes in series with Dynalene flowing through P38 and then directly through P01. The slower cooling times based on P01 pipe temperatures is therefore conservative.

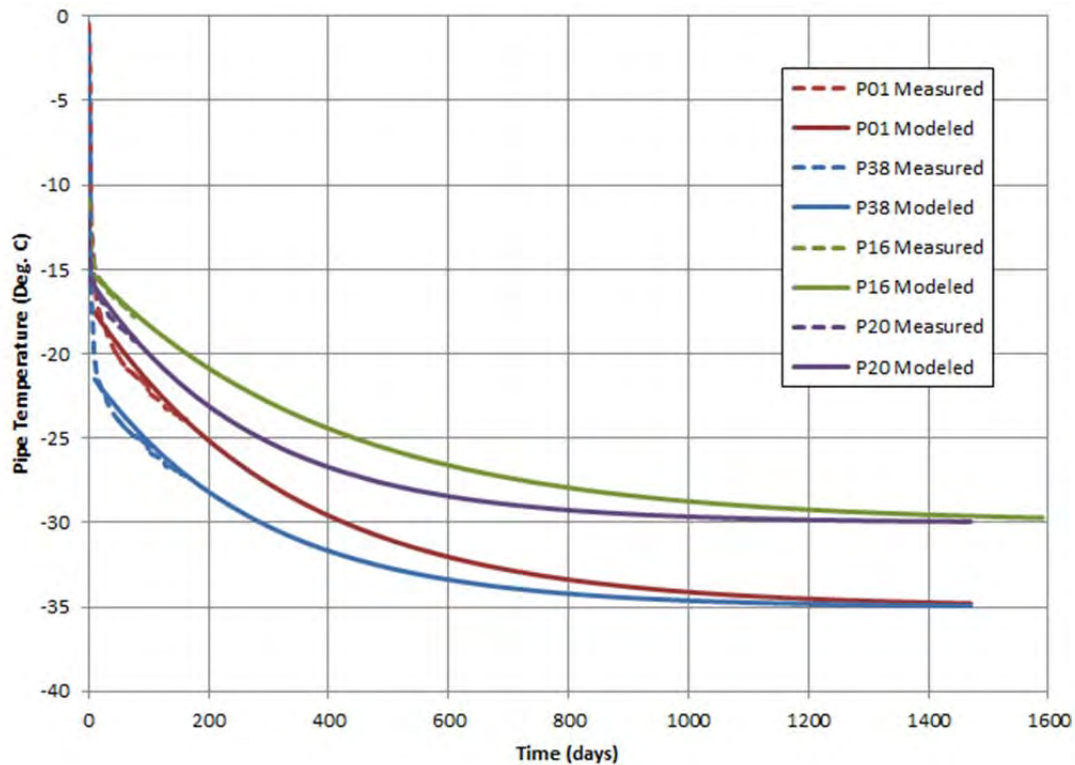
Figure 8-23 provides the daily averaged pipe temperatures for P01 over the first 165 days of the FOS. Pipe temperatures intermittently increased at various points in the study due to power outages and ambient air temperature above about 20 °C causing a temporary increase in Dynalene supply temperature at the plant. Prior to curve fitting, the data during periods of disruptions were eliminated from the data set.

Figure 8-24 provides a summary of the modeled pipe temperatures for the range of active freeze pipes and hybrid thermosyphons. For the hybrid thermosyphons, only Groups F and G with 77 days of data were evaluated for the simulations and the days available are during active operation only, no passive heat extraction is included in the simulation. As a result, there is some uncertainty in the hybrid thermosyphon prediction times.



Source File: FOS10mWallPredictionModelInputs.1CS019.018.rev00.pm.xlsx

Figure 8-23: Comparison of measured and modeled pipe temperatures for P01



Source File: FOS10mWallPredictionModelInputs.1CS019.018.rev00.pm.xlsx

Figure 8-24: Comparison of modeled pipe temperatures

8.7.2 Effect of Arsenic Chamber Offset

Table 8-10 provides the results of the sensitivity analysis of time to establish the freeze wall for active freeze pipes and hybrid thermosyphons over the typical range of diffusivities (0.15 to 0.19 m²/day) both with and without the arsenic chamber present at a 7 m offset.

For the active freeze pipes, the initial freezing period ranges from 6.3 to 8.7 months with a 7 m offset, and 8.5 to 11.7 months with no arsenic chamber. For the 7m offset, the initial freeze period is less than the 10 months predicted in the conceptual design.

For the hybrid thermosyphon, the initial freezing period (for active heat extraction only) ranges from 8.0 to 10.5 months with a 7 m chamber offset and 11.2 to 15.1 months with no arsenic chamber present.

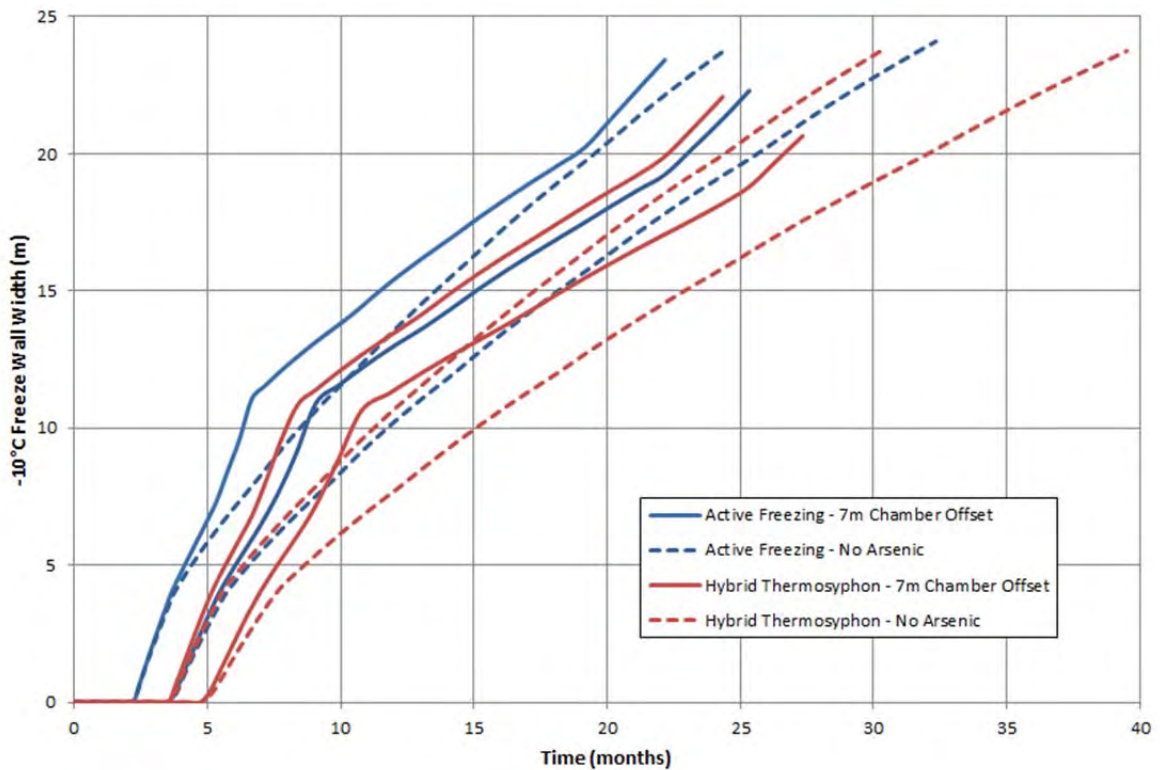
Exclusion of the arsenic chamber increased the initial freezing period by an average of 38%.

Table 8-10: Effect of Arsenic Chamber on Predicted time to reach -10 °C criterion (months)

	7 m offset from Chamber		No Chamber	
	Diffusivity 0.19 m ² /day	Diffusivity 0.15 m ² /day	Diffusivity 0.19 m ² /day	Diffusivity 0.15 m ² /day
Group A – P01	7.3	8.7	10	11.7
Group A – P38	6.3	7.5	8.5	10.1
Group F – P16	8.9	10.5	12.9	15.1
Group G – P20	8.0	9.5	11.2	13.2

Source File: FOS10mWallPredictionResults.1CS019.018.rev00.pm.xlsx

Figure 8-25 plots the range of -10 °C freeze wall thickness (measured between pipes) versus time for each simulation. For simulations without the arsenic chamber, the rate of wall thickness development decreases with time. For simulations with the chamber, the wall develops quicker due to the insulating effect of the chamber. Once the -10 °C freeze front reaches the chamber, the rate of thickness increase reduces significantly. This occurs in the graph at a wall thickness of approximately 11 m and confirms that the 7 m offset is near the optimal distance from the chamber wall.



Source File: FOS10mWallPredictionModelResults.1CS019.018.rev00.pm.xlsx

Figure 8-25: Freeze wall thickness versus time with and without 7 m chamber offset and without

8.7.3 Effect of Pipe Spacing

Table 8-11 provides the results of the pipe spacing sensitivity analysis for active freeze pipes and hybrid thermosyphons over the typical range of diffusivities (0.15 to 0.19 m²/day).

The arsenic chamber was excluded from the simulations. In each freeze area, due to the enclosure of contaminated drifts, irregular stope/chamber geometries, and access issues, there will likely be a portion of each freeze area that will be further than 7 m from the arsenic and not receive the insulating effect. This outside area would control the completion time of the 10 m wide, -10 °C freeze shell.

For all cases, increasing the pipe spacing from 4 to 5 m increased the initial freezing period by an average of 17% (range 15 to 19%). Increasing the pipe temperature from 5 to 6 m, further increased the freeze pipe by 16% (range 15 to 17%).

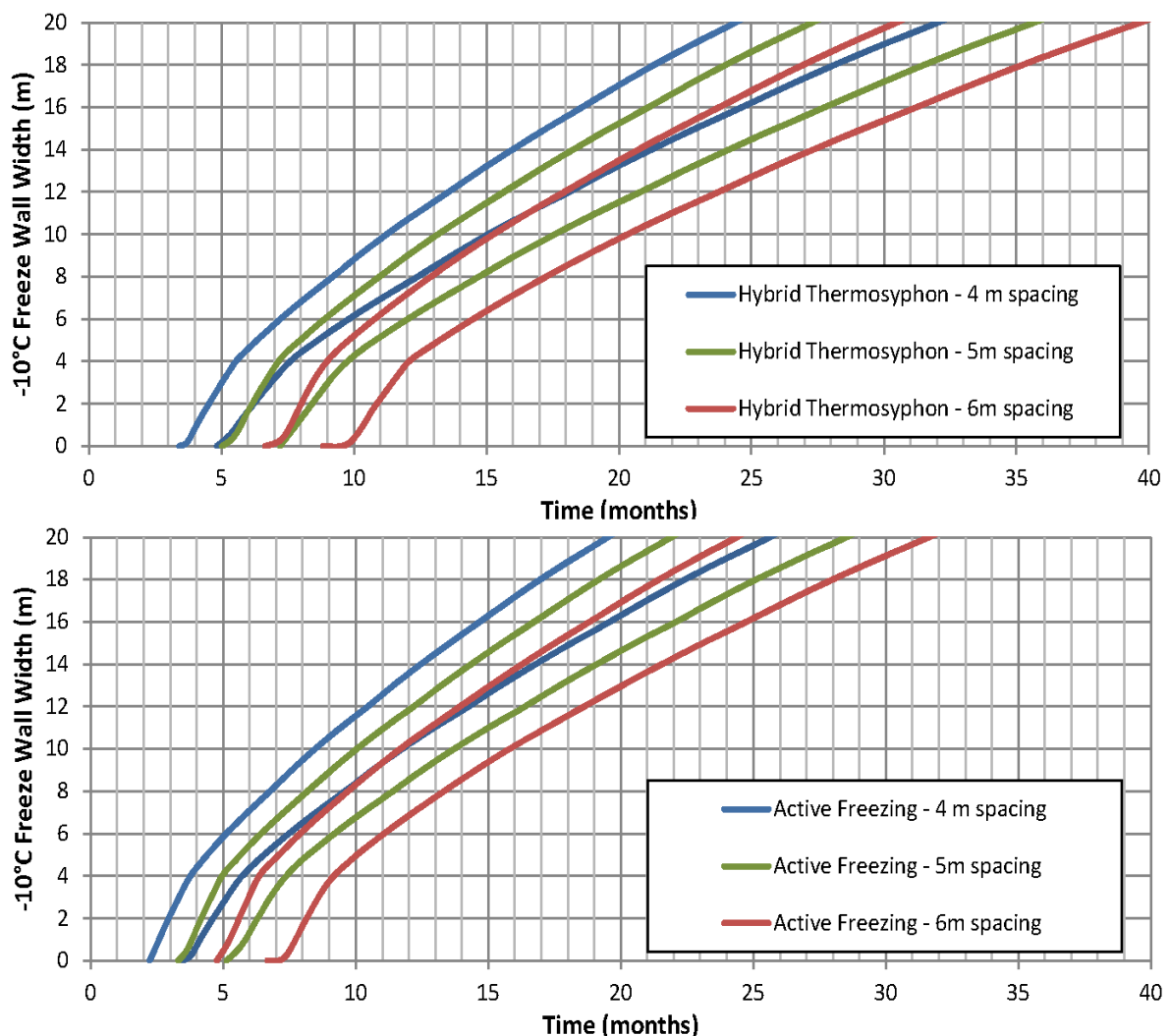
Table 8-11: Effect of Pipe Spacing on Predicted time to reach -10 °C criterion (months)

	4m Pipe Spacing (No chamber)		5m Pipe Spacing (No chamber)		6m Pipe Spacing (No chamber)	
	Diffusivity 0.19 m ² /day	Diffusivity 0.15 m ² /day	Diffusivity 0.19 m ² /day	Diffusivity 0.15 m ² /day	Diffusivity 0.19 m ² /day	Diffusivity 0.15 m ² /day
Group A – P01	10	11.7	11.7	13.7	13.5	15.8
Group A – P38	8.5	10.1	10.0	11.9	11.7	13.9

Group F – P16	12.9	15.1	15.1	17.6	17.4	20.3
Group G – P20	11.2	13.2	13.2	15.5	15.3	17.9

Source File: FOS10mWallPredictionResults.1CS019.018.rev00.pm.xlsx

Figure 8-26 plots the range of predicted times of freeze wall widths at each pipe spacing for both the active freeze pipes and hybrid thermosyphons. Using the 12 month target for establishing the initial freeze criteria adopted in the conceptual design, the plots show that for the active freeze pipes, a 5 m pipe spacing can achieve the target based for the average freeze pipe performance. For the hybrid thermosyphons, the modeling results indicates that a 4m pipe spacing may not meet the 12 month target in all areas, with results ranging from 11 to 15 months. However, inclusion of passive heat extraction during the winter months would reduce the predicted freeze times. There is not sufficient data from the freeze study at this time to assess the hybrid (active plus passive) performance during the winter months.



Source File: FOS10mWallPredictionModelResults.1CS019.018.rev00.pm.xlsx

Figure 8-26: -10°C Freeze wall thickness for different pipe spacing

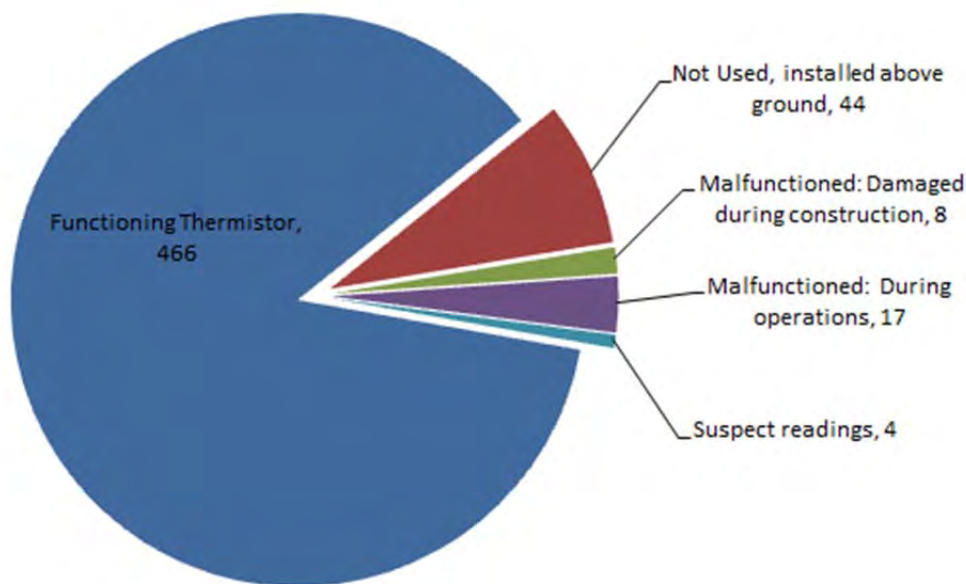
8.8 Instrumentation Reliability

This section presents a preliminary reliability assessment of the number of malfunctioned instrumentation up to the end of August 2011, following a half year of operation. Where applicable, the suspected causes of failure are noted. Assessed are the in-ground thermistors and vibrating wire piezometers, and above ground flow meters and RTDs.

8.8.1 Thermistors

Thermistor strings were installed in 34 instrumentation holes and 15 freeze holes (49 total). Each thermistor strings has 11 sensors for a total of 539 sensors.

The status of each thermistor is summarized in Figure 8-27. Of the thermistors ordered for the project, 86% were installed in the ground and are currently functioning as expected. Additionally, 8% of the thermistors were installed above ground and are currently not in use. This occurred either due to: shorter than design drill holes, typically from sloughing, or strings being installed in a drill-hole different from its assigned hole. Swapping of thermistor string assignments occurred when a drill hole was completed and ready for a string to be installed, but the assigned string had not yet been delivered to site.



Source File: FOSInstrumentationIssues.1CS019.018.rev00.xlsx

Figure 8-27: Thermistor Reliability Assessment

During installation, 8 thermistor sensors (1% of the total) were damaged. The damaged sensors occur in four separate holes and are typically at near the bottom of the hole and were likely crushed or damaged by being pressed against the side of the drill-hole.

Since the start of ground freezing, 17 sensors have malfunctioned (3.5% of the functioning sensors). The installed sensors are temperature sensitive resistors with a temperature range of +15 °C to -45 °C. Resistance increases with decreasing temperature. When a sensor malfunctions, the recorded value is typically -45 °C (highest resistance) this indicates that no current passes through the resistor

and that either the cable or the resistor has been severed. The damage may be caused by thermal expansion and contraction of water during freezing, but there is no significant evidence of sensors malfunctioning near 0 °C. Of the 17 sensors, 7 have malfunctioned near a temperature of 0 °C. However, this could be coincidence as during the first few months of the study, most sensors in the bedrock have passed through 0 °C.

There were 4 sensors that record suspect readings. These readings are generally temperatures a few degrees different than values immediately above and below on the string with no known cause for the discrepancy.

8.8.2 Vibrating Wire Piezometers

Piezometer strings were installed in instrumentation holes S34 and S37. Each string contains 10 piezometers. Due to the restricted number of cable terminations available in the instrumentation building, only the bottom 3 piezometers have been terminated on each string and are providing readings. (As a lower piezometer becomes frozen during the dust wetting process, it will be disconnected and the next higher piezometer will be connected.)

There is currently no pooled water within Chamber 10 detected by the piezometers or the water level is below the piezometers. As a result, there has been no change to instrumentation readings since data has been recorded.

There are no known issues with the vibrating wire piezometer instrumentation.

8.8.3 Flow Meters

On the active freeze distribution system, flow meters monitor the Dynalene flow rate through each freeze pipe, distribution loop and total flow out of the plant. On the hybrid thermosyphon system, two mass flow meters are installed on each thermosyphon: one for each refrigerant coil loop.

As of the end of August 2011, all flow meters on the active freeze distribution system have functioned as expected throughout the study.

On the thermosyphon refrigerant distribution system, a coriolis mass flow meter (CoriolisMaster FCM2000) is installed on each refrigerant loop for a total of 24 flow meters. Problems have been encountered on two of the meters:

- Pipe P23, Coil A (Group F): On May 30, 2011 the flow meter started to record zero values. No flow was occurring through the coil due to a parameter error in the programming of the coil. The coil was reactivated on June 19, 2011.
- Pipe P16, Coil B (Group G): On Sept 13, 2011 the flow meter stopped recording data. At the time of writing, the coil has been turned off and the flow meter sent for repairs.

8.8.4 Resistance Temperature Detectors (RTDs)

The 158 RTDs were installed and are regularly monitored as part of the FOS, 6 for each hybrid thermosyphon, 2 for each active freeze pipes and 4 at the Startec freeze plant. All RTDs are functioning since the start of ground freezing except for the P15 Dynalene supply temperature RTD that is not recording any data. For analysis purposes, the supply temperature of pipe P12 is used as a substitute.

On the underground freeze pipe U07, the temperature supply and return RTDs were terminated in reverse order. The readings were corrected in the heat flux calculations, and the RTD terminations were corrected on May 24, 2011.

8.8.5 Power Meters

To monitor power consumption, three power meters are present at freeze plants: one at the AFCI plant and two at the Startec plant.

The power meter in the AFCI plant is equipped with an analog signal output. There are no known issues with this instrumentation.

The Startec plant power meters include a spinning disc that emits a pulse to the PLC every 10 kWh. The PLC counts the pulses and records the cumulative daily and monthly totals. It was determined in September 2011 that the manual recordings of power consumption at the Startec plant did not match values on the historian. The fact that not all pulses are being counted by the PLC is thought to be the main contributing factor. The issue is currently under investigation by AECOM for reconciliation. It will not be possible to reconstruct the power log although it may be possible to make an approximation. NOTE FOR DRAFT: At the time of writing the issue is under investigation.

From July 13 to July 20, 2011, no power readings were recorded at the Startec plant. On July 20, the power monitoring system was adjusted by AECOM and data acquisition resumed.

9 Summary of Findings to Date

Although the ground freezing is still in its early stages with the initial ground freezing criteria not yet achieved, the FOS has provided several important findings to date. These findings are summarized in the bullets below. Section references are noted for further details.

9.1 Data Management

Based on the issues encountered in the data collection and management of the FOS to date, the following recommendations are recommended for the future freeze program (Section 6.2):

- No data compression should be performed on the raw data.
- A common time interval should be established for all parameters that are required in the same calculation eliminate interpolation between data points.
- Instantaneous power consumption data should be tracked as it is for the AFCI plant.
- Exception rules should be periodically reviewed and adjusted to reduce the overall quantity of data collected. The first review should be completed with the first couple of weeks following the start of operations. Subsequent reviews may be completed every six months thereafter.
- Ensure instrumentation and data management systems are commissioned and all desired data is verified before start of freezing.

9.2 Ground Freeze Progress

- Section 7 provides an illustration of the approximate freeze progress to September 8, 2011 after approximately six months following the start of ground freezing operations. The ground

freezing for the active freeze pipes has progressed further than anticipated to date compared to the conceptual design. The quicker performance is due to differences in the material properties of the bedrock.

- Even without the activation of freeze pipes at the northern end southern end of the study, the 0 °C isotherm has surrounded the chamber on all sides.

9.3 Design Parameters

- Results of the mineralogy assessment indicate that the thermal properties of the bedrock on the west side of the test are significantly different from those on the east side. On both sides, the thermal conductivities are higher than used in the conceptual design. The typical thermal conductivity at the FOS was selected as $400 \text{ kJ m}^{-1} \text{ day}^{-1} \text{ }^{\circ}\text{C}^{-1}$ and was found to range from 230 to $485 \text{ kJ m}^{-1} \text{ day}^{-1} \text{ }^{\circ}\text{C}^{-1}$ (Section 8.1.1).
- Ground temperatures measured to date indicate that the bedrock has a higher thermal diffusivity (i.e., it cools more rapidly) than assumed in the conceptual design. Typical bedrock diffusivities ranged from 0.15 to $0.19 \text{ m}^2/\text{day}$. The conceptual design diffusivity was based on model calibration of the experimental thermosyphon on the north end of the Giant Mine properties. The diffusivity difference between the two sites is due to differences in the bedrock material properties (Section 8.1.2).
- The Coefficient of Performance (COP) is the ratio of the estimated heat extraction to the measured power input, and is a measure of cooling system efficiency. Higher values indicate better performance. The COP for the AFCL freeze plant for active operation to date has ranged between 1.0 and 1.3 when all hybrid thermosyphons are operating. These values do not include passive heat removal. Due to the uncertainty of the power consumption at the Startec plant, the COP for the Startec plant is not substantiated at this time (Section 8.1.5).
- Heat transfer coefficients for the month of September 2011 have ranged from 2,300 to $4,100 \text{ kJ m}^{-1} \text{ day}^{-1} \text{ }^{\circ}\text{C}^{-1}$ for 4 inch freeze pipes and $6,700 \text{ kJ m}^{-1} \text{ day}^{-1} \text{ }^{\circ}\text{C}^{-1}$ for 3 inch freeze pipes. The coefficients are slowly decreasing as the Dynalene temperature in the pipe decreases and are expected to level off. The theoretical expected heat transfer coefficients are 3,000 and $5,400 \text{ kJ m}^{-1} \text{ day}^{-1} \text{ }^{\circ}\text{C}^{-1}$ for the 4 inch and 3 inch freeze pipes respectively (Section 8.1.6).
- Pipe temperature and calculated ground heat extraction rate results indicate that:
 - The 3 inch freeze pipes are performing as well as the 4 inch freeze pipes (Section 8.4).
 - The 2.5 inch hybrid thermosyphons are performing as well as the 4 inch hybrid thermosyphons (Section 8.2).
- Updated model simulations using the revised study parameters indicate that for active freezing, 5 m pipe spacing will be able to achieve the initial freeze criteria within 12 months (Section 8.7).

9.4 Comparison to Study Objectives

The specific objectives of the freeze optimization study were outlined in the FOS Interim As-Built Report (2010a). Table 9-1 lists the objectives and how the FOS results to date have met each objective.

Table 9-1: Comparison to Study Objectives

Study Objective	Status of Objective
1. Demonstrate Large Scale Ground Freezing	
<ul style="list-style-type: none"> The project will provide a demonstration of ground freezing at a scale and level of complexity relevant to subsequent design. 	<p>Components of the FOS relevant to the main freeze program are numerous. Some key examples are:</p> <ul style="list-style-type: none"> - Identifying contamination during site preparation - Encountering bedrock during site preparation - Mitigating contamination during site preparation - Installing conductor and casing pipes - Drilling into and through open drifts - Applying drill hole survey methods - Drilling into the top of an arsenic storage area - Installing conductor and casing pipes - Installing instrumentation on pipes - Installing instrumentation inside the Chamber - Applying drill hole grouting methods
<ul style="list-style-type: none"> The project will be accessible to local stakeholders to show how the method would be applied to freeze all of the underground arsenic trioxide. 	<p>Publication of FOS data reports to will be accessible to local stakeholders.</p>
2. Estimate Parameters Needed for Design	
<ul style="list-style-type: none"> The project will allow the collection of data that can be used to improve estimates of parameters that will govern the full-scale design. Examples of such parameters are the thermal conductivity of the bedrock, overburden materials, arsenic trioxide dust, the rates of power consumption during the active freezing stage, and the efficiencies (coefficient of performance or COP) of each freezing method. 	<p>The FOS has provided information about some parameters while others are to be determined as the study continues. To date, evaluation and parameter identification methods are in place. Parameters that involve methods developed to improve estimates include:</p> <ul style="list-style-type: none"> - Thermal conductivity of the rock - Efficiencies of the freeze variants - Freeze pipe size - Efficiencies of the freeze plants - Rates of heat extraction - Estimating the thermal conductivity of the arsenic dust and other in Chamber have not been part of the FOS to date <p>However at the time of writing, the power data were under review and power usage and efficiency values could not be estimated conclusively. They will not be available until discrepancies in power data are resolved.</p>
<ul style="list-style-type: none"> Improved estimates of those parameters will allow optimization of the designs for the remaining stopes and chambers. An example of the optimization process will be selecting the optimal trade-offs between freeze pipe spacing, cooling power and freezing time. 	<p>The trade-off studies for design optimization have not been completed at this time. There is currently insufficient data with respect to power consumption and year-round hybrid thermosyphon performance.</p>

3. Test Implementation Methods The project will allow several methods that could be used in the full-scale freezing to be tested.	
<ul style="list-style-type: none"> Methods for active, passive and hybrid-passive freezing. 	All freeze methods mentioned have been installed at the FOS. Furthermore, they have been installed in variants to learn their effect on freeze performance. Active freezing is installed with the Dynalene system. Passive and hybrid-passive freezing capabilities are installed with AFCI's thermosyphon system.
<ul style="list-style-type: none"> Methods to convert initial active or hybrid-passive freezing systems to long-term passive freezing. 	The conversion of the initial freezing systems to a passive system for long-term freeze maintenance has not been tested. The FOS construction allows for several conversion options including: <ul style="list-style-type: none"> Standard conversion of active freeze pipes to thermosyphons by inserting thermosyphon pipes into active freeze pipes Leaving the hybrid thermosyphons in place and disconnecting the heat exchange loops Removing the collar arrangement from active freeze pipes and welding thermosyphon condensers directly onto the active freeze pipes
<ul style="list-style-type: none"> Methods to sample and test contaminated soils (that will be removed from the project area). 	The sampling and testing of contaminated soils was performed during site preparation. A standardized grid and sampling protocol was used to gather samples after excavation. The samples were analyzed for statistical significance with respect to grid size. The results are documented in Appendix A.
<ul style="list-style-type: none"> Methods to repair or replace inaccessible underground plugs and bulkheads. 	This objective is outside SRK's terms of reference for the FOS. Design of drift plugs to be completed by AECOM.
<ul style="list-style-type: none"> Methods to drill holes for freeze pipes and instrumentation. 	Percussion, mud rotary, and diamond drilling technologies were used to drill holes on the surface for freeze pipes and instrumentation. Underground holes, for both freeze pipes and instrumentation, were drilled with a variation of percussion drilling. Drilling evaluation is covered in the Interim As-Built Report (2010a) by SRK.
<ul style="list-style-type: none"> Methods and materials for freeze pipes. 	This objective is outside SRK's terms of reference for the FOS.
<ul style="list-style-type: none"> Methods and materials for downhole instrumentation. 	At the time of writing, a large majority of the downhole instrumentation is functional. The specification for the downhole instrumentation is satisfactory, however, the method and arrangement for installation would reduce lost readings (see Section 8.9).
4. Develop Data Handling Methods The project will include collection of monitoring data of a scale and complexity similar to what will be needed during full-scale implementation. Methods to collect manage the data will be developed and tested.	
<ul style="list-style-type: none"> Testing of sensors to measure ground temperatures and freezing system performance. 	SRK specified the temperature sensors and piezometers installed in drill holes and in the Chamber 10. Temperature readings are performing well. Piezometer readings are yet to be verified; they are reading close to zero as there may be no water in the chamber to detect. Defective readings are thought to be largely due to installation conditions and onset of freezing. Specification of sensors above ground was provided by others.
<ul style="list-style-type: none"> Development and testing of a data capture system. 	Details of the data capture system are described in Section 6.

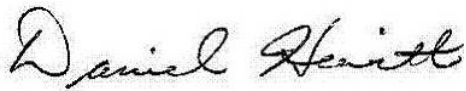
<ul style="list-style-type: none"> • Development and testing of a process control system. 	<p>Design of the data acquisition system was outside SRK's scope. To date, process control has been focused on the freezing experiment, but the experience gained is relevant to operation of a "normal" freezing system.</p>
<ul style="list-style-type: none"> • Development of a monitoring database. 	<p>Details of the database developed for monitoring of instrumentation is described in Section 0.</p>
<ul style="list-style-type: none"> • Development and testing of data interpretation models for each stage of the freezing. 	<p>2D and 3D models have been successfully calibrated to mimic thermal behaviour of the FOS in its current state. Further modeling would be required for estimation of the arsenic properties, wetting, freezing through to frozen block status, and long term monitoring and maintenance.</p>
<p>5. Project Procurement and Delivery Methods</p> <p>The development of procurement and delivery methods is key to the logistical success of the freeze program. The FOS to date has had design, construction and operation phases upon which experience has been gained to provide insights into better ways to supply goods and services. This includes management of materials as well as human resources.</p>	
<ul style="list-style-type: none"> • The project will require a level of engineering design and construction management that will provide insights into methods to deliver the full-scale project. Examples include the roles of technical advisor, design engineer, construction manager, specialist contractors and the relationships with PWGSC and INAC oversight. 	<p>This objective is outside SRK's terms of reference for the FOS.</p>
<ul style="list-style-type: none"> • The project will require procurement of most component types that will be needed for the full-scale freeze, and will allow examination and documentation of the needs for full-scale procurement. Examples include the lead time needed for critical components, the responsiveness of suppliers, the need to bundle or un-bundle related items, and the range of options that need to be allowed for in each category of material or process. 	<p>This objective is outside SRK's terms of reference for the FOS.</p>
<p>6. Examine Unknown Unknowns</p> <p>The preceding objectives represent "known unknowns," i.e., things we know we don't know. The project will also undoubtedly provide insights into "unknown unknowns," i.e., things that we currently don't imagine that we need to know. It is preferable to deal with as many of these considerations as possible in this study, so their risks to the full-scale project can be minimized</p>	
<ul style="list-style-type: none"> • No specific items identified 	<p>Several examples arose during construction, including the difficulty of managing multiple contractors working in a restricted area, the challenges encountered in designing, procuring, integrating SCADA for freeze plants and commissioning the data management system.</p>

This report, "Giant Mine Freeze Optimization Study – Initial Findings Report", has been prepared by SRK Consulting (Canada) Inc.

Prepared by



Peter Mikes, P. Eng.
Senior Consultant



Dan Hewitt, P. Eng.
Principal Consultant

Reviewed by



Daryl Hockley, P. Eng.
Principal Consultant

All data used as source material plus the text, tables, figures, and attachments of this document have been reviewed and prepared in accordance with generally accepted professional engineering and environmental practices.

10 References

Arctic Foundations of Canada Inc, 2011. Personal communications with John Jardine.

Clauser, C. and Huenges, E. (1995). Thermal Conductivity of Rocks and Minerals. In Rock Physics and Phase Relations: a Handbook of Physical Constants, Vol. 3 pp. 105-126.

Newman, G.P. and Lam, L. 2000. Simple application of a convective heat transfer boundary in a FEM freezing analysis. Ground Freezing 2000, Proceedings of the International Symposium on Ground Freezing and Frost Action in Soils, Louvain-La-Neuve, Belgium, 11-13 September, pp. 205-216.

SoilVision Systems, 2009. SVOOffice 2009 User's Manual. SoilVision Systems, Ltd. Saskatoon, Sask.

SRK, 2010a. Giant Mine Freeze Optimization Study Interim As-Built Report. Prepared for: Public Works and Government Services Canada. SRK Project Number 1CS019.012. August, 2010.

SRK, 2010b. Draft Memorandum, "Giant – FOS Thermal Modeling Results and Sensitivity Analysis". Memo to file. SRK Project Number 1CS019.012.007.

SRK, 2006. "Giant Mine Remediation Project, Conceptual Engineering for Ground Freezing", Prepared for the Giant Mine Remediation Project Team, Department of Indian Affairs and Northern Development. January, 2006.